ASC Report No. 12/2010

Convergence of Adaptive BEM for some Mixed Boundary Value Problem

Markus Aurada, Samuel Ferraz-Leite, Petra Goldenits, Michael Karkulik, Markus Mayr, Dirk Praetorius

Institute for Analysis and Scientific Computing
Vienna University of Technology — TU Wien
www.asc.tuwien.ac.at ISBN 978-3-902627-03-2

Most recent ASC Reports

11/2010 *Mario Bukal, Ansgar Jüngel, Daniel Matthes*
Entropies for Radially Symmetric Higher-Order Nonlinear Diffusion Equations

10/1010 *Karl Rupp, Ansgar Jüngel, Karl-Tibor Grasser*
Matrix Compression for Spherical Harmonics Expansions of the Boltzmann Transport Equation for Semiconductors

9/2010 *Markus Aurada, Samuel Ferraz-Leite, Dirk Praetorius*
Estimator Reduction and Convergence of Adaptive BEM

8/2010 *Robert Hammerling, Othmar Koch, Christa Simon, Ewa B. Weinmüller*
Numerical Solution of singular Eigenvalue Problems for ODEs with a Focus on Problems Posed on Semi-Infinite Intervals

7/2010 *Robert Hammerling, Othmar Koch, Christa Simon, Ewa B. Weinmüller*
Numerical Solution of Singular ODE Eigenvalue Problems in Electronic Structure Computations

6/2010 *Markus Aurada, Michael Feischl, Dirk Praetorius*
Convergence of Some Adaptive FEM-BEM Coupling

5/2010 *Marcus Page, Dirk Praetorius*
Convergence of Adaptive FEM for some Elliptic Obstacle Problem

4/2010 *Ansgar Jüngel, Josipa-Pina Milišić*
A Simplified Quantum Energy-Trans port Model for Semiconductors

3/2010 *Georg Kitzhofer, Othmar Koch, Gernot Pulverer, Christa Simon, Ewa Weinmüller*
The New MATLAB Code bvpsuite for the Solution of Singular Implicit BVPs

2/2010 *Maike Löhndorf, Jens Markus Melenk*
Wavenumber-explicit hp-BEM for High Frequency Scattering

Institute for Analysis and Scientific Computing
Vienna University of Technology
Wiedner Hauptstraße 8–10
1040 Wien, Austria

E-Mail: admin@asc.tuwien.ac.at
WWW: http://www.asc.tuwien.ac.at
FAX: +43-1-58801-10196

ISBN 978-3-902627-03-2

© Alle Rechte vorbehalten. Nachdruck nur mit Genehmigung des Autors.

ASC TU WIEN

CONVERGENCE OF ADAPTIVE BEM FOR SOME MIXED BOUNDARY VALUE PROBLEM

M. AURADA, S. FERRAZ-LEITE, P. GOLDENITS, M. KARKULIK, M. MAYR, AND D. PRAETORIUS

Abstract. For a boundary integral formulation of the 2D Laplace equation with mixed boundary conditions, we consider an adaptive Galerkin BEM based on an $(h-h/2)$-type error estimator. We include the resolution of the Dirichlet, Neumann, and volume data into the adaptive algorithm. In particular, an implementation of the developed algorithms has only to deal with discrete integral operators. We prove that the proposed adaptive scheme leads to a sequence of discrete solutions, for which the corresponding error estimators tend to zero. Under a saturation assumption for the non-perturbed problem which is observed empirically, the sequence of discrete solutions thus converges to the exact solution within the energy norm.

1. Introduction

The $(h-h/2)$-error estimation strategy is a well-known technique to derive a posteriori estimators for the error $|||\mathbf{u}-\mathbf{U}_\ell|||$ in the energy norm; see [21] in the context of ordinary differential equations, and the overview article of Bank [5] or the monograph [1, Chapter 5] in the context of the finite element method: Let $\mathcal{X}_\ell$ be a discrete subspace of the energy space $\mathcal{H}$ and let $\widehat{\mathcal{X}}_\ell$ be its uniform refinement. With the corresponding Galerkin solution $\mathbf{U}_\ell$ and $\widehat{\mathbf{U}}_\ell$, the canonical $(h-h/2)$-*error estimator*

$$\eta_\ell := |||\widehat{\mathbf{U}}_\ell - \mathbf{U}_\ell||| \tag{1.1}$$

is a computable quantity [13] which can be used to estimate $|||\mathbf{u}-\mathbf{U}_\ell|||$, where $\mathbf{u}\in\mathcal{H}$ denotes the exact solution.

For finite element methods (FEM), the energy norm, e.g., $|||\cdot||| = \|\nabla(\cdot)\|_{L^2(\Omega)}$ provides local information, which elements of the underlying mesh should be refined to decrease the error effectively. For boundary element methods (BEM), the energy norm $|||\cdot|||$ is (equivalent to) a fractional order (and possibly negative) Sobolev norm and typically does not provide local information. In [16, 18], localized variants of η_ℓ were introduced for certain weakly-singular and hypersingular integral equations. In [15, 16] the equivalence of η_ℓ to hierarchical two-level error estimators from [22, 24, 27] and averaging error estimators from [8, 9, 10] has been proven.

Recently [17], convergence of some $(h-h/2)$-steered adaptive mesh-refinement has been proven for linear model problems in the context of FEM and BEM. In [3], the concept of estimator reduction has been introduced to analyze convergence of anisotropic mesh-refinement steered by $(h-h/2)$-type or averaging-based error estimators for weakly-singular integral equations arising in 3D BEM. However, in [3, 17] it is assumed that the right-hand side of the integral equation is computed analytically.

In this work, we consider the so-called symmetric integral formulation of a mixed boundary value problem in 2D. Contrary to prior works, we include the approximation of the given Dirichlet, Neumann, and volume data into the a posteriori error estimate. Therefore, the proposed scheme deals with discrete integral operators only which can then

be approximated by means of hierarchical matrices [20] or the fast multipole method, cf. [28] and the references therein.

The proposed error estimator ϱ_ℓ is a sum of certain $(h-h/2)$-error estimators which control the discretization error, and certain data oscillation terms which control the consistency errors introduced by the data approximation. The estimator ϱ_ℓ is easily implemented and can be computed in linear complexity. In particular, it is part of the developed MATLAB BEM library `HILBERT` [2].

Using the concept of estimator reduction from [3], we even prove that the usual adaptive algorithm, steered by ϱ_ℓ, enforces $\lim_\ell \varrho_\ell = 0$. Under a saturation assumption, which is empirically observed in numerical experiments, this implies convergence $\lim_\ell \mathbf{U}_\ell = \mathbf{u}$ of the discrete solutions.

The remainder of this paper is organized as follows: Section 2 introduces the symmetric integral formulation of the model problem as well as the data-perturbed Galerkin formulation and states the main results of this work, where we first focus on homogeneous volume forces. In Section 3, we collect the essential preliminaries, namely the mapping properties of the involved integral operators as well as certain inverse estimates and approximation results. Section 4 introduces and analyzes the data oscillation terms as well as the proposed error estimator ϱ_ℓ. Our version of the adaptive mesh-refining algorithm is found in Section 5, and we prove convergence $\lim_\ell \varrho_\ell = 0$. In Section 6, we briefly sketch how the analysis can be generalized to non-homogeneous volume forces. Numerical experiments in Section 7 underline that the proposed adaptive algorithm performs very effectively in practice.

2. Model problem and analytical results

The aim of this section is to introduce the model problem, its integral formulation, and the Galerkin formulation. Moreover, we sketch our main results and give and overview on the results contained in this work.

2.1. Continuous model problem. In a first step, we consider the homogeneous mixed boundary value problem

$$\left\{ \begin{array}{rcll} -\Delta u &=& 0 & \text{in } \Omega, \\ u &=& u_D & \text{on } \Gamma_D, \\ \partial_n u &=& \phi_N & \text{on } \Gamma_N, \end{array} \right. \tag{2.1}$$

where $u_D : \Gamma_D \to \mathbb{R}$ and $\phi_N : \Gamma_N \to \mathbb{R}$ are given data and where the solution $u : \Omega \to \mathbb{R}$ is sought. The boundary $\Gamma := \partial\Omega$ of the bounded Lipschitz domain $\Omega \subset \mathbb{R}^2$ is split into (relatively open) Dirichlet and Neumann boundaries, which satisfy $\Gamma_D \cap \Gamma_N = \emptyset$, $\Gamma = \overline{\Gamma}_D \cup \overline{\Gamma}_N$, and $|\Gamma_D| > 0$. For technical reasons, we further assume $\operatorname{diam}(\Omega) < 1$, see Section 3.2 below. This problem is equivalently recast into the so-called symmetric boundary integral formulation

$$A \begin{pmatrix} u_N \\ \phi_D \end{pmatrix} = (1/2 - A) \begin{pmatrix} u_D \\ \phi_N \end{pmatrix} =: F \text{ with operator matrix } A := \begin{pmatrix} -K & V \\ W & K' \end{pmatrix}. \tag{2.2}$$

Here, V is the simple-layer potential, K is the double-layer potential with adjoint K', and W is the hypersingular integral operator. In this formulation, we fix arbitrary extensions $u_D : \Gamma \to \mathbb{R}$ and $\phi_N : \Gamma \to \mathbb{R}$ which satisfy $(u_D, \phi_N) \in H^{1/2}(\Gamma) \times H^{-1/2}(\Gamma)$ and seek a solution $\mathbf{u} := (u_N, \phi_D) \in \mathcal{H} := \widetilde{H}^{1/2}(\Gamma_N) \times \widetilde{H}^{-1/2}(\Gamma_D)$.

Let $\langle \cdot\,, \cdot \rangle$ denote the L^2-scalar product which is extended to duality between $\widetilde{H}^{-1/2}(\Gamma_D)$ and $H^{1/2}(\Gamma_D)$ and between $H^{-1/2}(\Gamma_N)$ and $\widetilde{H}^{1/2}(\Gamma_N)$. Note that A is a linear and continuous operator from $\mathcal{H}$ to $\mathcal{H}^* = H^{1/2}(\Gamma_D) \times H^{-1/2}(\Gamma_N)$, where duality is understood via

(2.3)
$$\langle (v_D, \psi_N), (v_N, \psi_D) \rangle_{\mathcal{H}^* \times \mathcal{H}} := \langle \psi_N, v_N \rangle + \langle \psi_D, v_D \rangle \text{ for all } (v_N, \psi_D) \in \mathcal{H},\ (v_D, \psi_N) \in \mathcal{H}^*.$$

In particular, A induces a continuous bilinear form on $\mathcal{H}$, namely

$$\begin{aligned} \langle\!\langle (u_N, \phi_D), (v_N, \psi_D) \rangle\!\rangle &:= \langle A(u_N, \phi_D), (v_N, \psi_D) \rangle_{\mathcal{H}^* \times \mathcal{H}} \\ &= \langle W u_N + K' \phi_D, v_N \rangle + \langle \psi_D, -K u_N + V \phi_D \rangle. \end{aligned} \tag{2.4}$$

Clearly, $\langle\!\langle \cdot\,, \cdot \rangle\!\rangle$ is non-symmetric. Nevertheless, $|\!|\!| (u, \phi) |\!|\!| := \langle\!\langle (u, \phi), (u, \phi) \rangle\!\rangle^{1/2}$ defines an equivalent norm on $\mathcal{H}$ and, in particular, $\langle\!\langle \cdot\,, \cdot \rangle\!\rangle$ is elliptic, see Section 3.4 below. Therefore, the Lax-Milgram lemma proves the existence and uniqueness of the solution $\mathbf{u} = (u_N, \phi_D) \in \mathcal{H}$ of the variational form

$$\langle\!\langle \mathbf{u}, \mathbf{v} \rangle\!\rangle = \langle F, \mathbf{v} \rangle_{\mathcal{H}^* \times \mathcal{H}} \quad \text{for all } \mathbf{v} = (v_N, \psi_D) \in \mathcal{H}. \tag{2.5}$$

2.2. Galerkin discretization. We consider the lowest-order Galerkin discretization of (2.5) with discrete space

$$\mathcal{X}_\ell := \mathcal{S}^1_0(\mathcal{E}_\ell|_{\Gamma_N}) \times \mathcal{P}^0(\mathcal{E}_\ell|_{\Gamma_D}) \subset \widetilde{H}^{1/2}(\Gamma_N) \times \widetilde{H}^{-1/2}(\Gamma_D) =: \mathcal{H} \tag{2.6}$$

Here, $\mathcal{E}_\ell := \{E_1, \dots, E_N\}$ is a partition of Γ, and $\mathcal{E}_\ell|_{\Gamma_N}$ and $\mathcal{E}_\ell|_{\Gamma_D}$ are the induced partitions of Γ_N and Γ_D. Moreover, $\mathcal{P}^0(\mathcal{E}_\ell|_{\Gamma_D})$ denotes the space of piecewise constant functions on Γ_D, and $\mathcal{S}^1_0(\mathcal{E}_\ell|_{\Gamma_N})$ denotes the space of continuous and piecewise affine functions that vanish on $\overline{\Gamma}_D = \Gamma \backslash \Gamma_N$.

Note that the Lax-Milgram lemma also applies for $\mathcal{X}_\ell$, and $\mathbf{U}^\star_\ell = (U^\star_{N,\ell}, \Phi^\star_{D,\ell}) \in \mathcal{X}_\ell$ denotes the uniquely determined Galerkin solution of

$$\langle\!\langle \mathbf{U}^\star_\ell, \mathbf{V}_\ell \rangle\!\rangle = \langle F, \mathbf{V}_\ell \rangle \quad \text{for all } \mathbf{V}_\ell = (V_{N,\ell}, \Psi_{D,\ell}) \in \mathcal{X}_\ell. \tag{2.7}$$

We stress that the Galerkin solution is quasi-optimal

$$|\!|\!| \mathbf{u} - \mathbf{U}_\ell |\!|\!| \le C_{\rm opt} \min_{\mathbf{V}_\ell \in \mathcal{X}_\ell} |\!|\!| \mathbf{u} - \mathbf{V}_\ell |\!|\!|, \tag{2.8}$$

where the constant $C_{\rm opt} > 0$ depends only on Γ.

However, since the right-hand side in (2.7) can hardly be evaluated numerically, we additionally approximate F by some appropriate F_ℓ. To that end, we assume additional regularity $u_D \in H^1(\Gamma) \subset C(\Gamma)$ and $\phi_N \in L^2(\Gamma)$ and define

$$F_\ell := (1/2 - A) \begin{pmatrix} I_\ell u_D \\ \Pi_\ell \phi_N \end{pmatrix}, \tag{2.9}$$

where $I_\ell : C(\Gamma) \to \mathcal{S}^1(\mathcal{E}_\ell)$ denotes the nodal interpolation operator and where $\Pi_\ell : L^2(\Gamma) \to \mathcal{P}^0(\mathcal{E}_\ell)$ denotes the L^2-projection onto the piecewise constants. Let $\mathbf{U}_\ell = (U_{N,\ell}, \Phi_{D,\ell}) \in \mathcal{X}_\ell$ be the uniquely determined solution of the perturbed Galerkin scheme

$$\langle\!\langle \mathbf{U}_\ell, \mathbf{V}_\ell \rangle\!\rangle = \langle F_\ell, \mathbf{V}_\ell \rangle \quad \text{for all } \mathbf{V}_\ell = (V_{N,\ell}, \Psi_{D,\ell}) \in \mathcal{X}_\ell. \tag{2.10}$$

We stress that all entries of the corresponding linear system can now be computed analytically. Moreover, another advantage is that the matrices which correspond to discrete integral operators, may now be easily approximated by, e.g., hierarchical matrix techniques [20] or the fast multipole method, cf. [28] and the references therein. The inclusion of the additional approximation error is neglected here, but it will be the topic of our future research.

2.3. A posteriori error estimation. In Section 4, we adapt and extend ideas from [4, 15, 16, 18] and provide the numerical analysis for the following simple a posteriori error estimator: Let $\widehat{\mathbf{U}}_\ell^\star = (\widehat{U}_{N,\ell}^\star, \widehat{\Phi}_{D,\ell}^\star) \in \widehat{\mathcal{X}}_\ell$ be the Galerkin solution (2.7) with respect to the uniform refinement $\widehat{\mathcal{E}}_\ell$ of $\mathcal{E}_\ell$. Under the saturation assumption

$$|||\mathbf{u} - \widehat{\mathbf{U}}_\ell^\star||| \le C_{\rm sat}\, |||\mathbf{u} - \mathbf{U}_\ell^\star||| \quad \text{with } C_{\rm sat} \in (0,1), \tag{2.11}$$

Theorem 4.1 states that the error estimator

$$\mu_\ell^\star := \big(\|h_\ell^{1/2}(\widehat{U}_{N,\ell}^\star - I_\ell \widehat{U}_{N,\ell}^\star)'\|_{L^2(\Gamma_N)}^2 + \|h_\ell^{1/2}(\widehat{\Phi}_{D,\ell}^\star - \Pi_\ell \widehat{\Phi}_{D,\ell}^\star)\|_{L^2(\Gamma_D)}^2\big)^{1/2} \tag{2.12}$$

provides a lower and upper bound for the unknown Galerkin error, namely

$$C_{\rm eff}^{-1}\, \mu_\ell^\star \le |||\mathbf{u} - \mathbf{U}_\ell^\star||| \le C_{\rm rel}\, \mu_\ell^\star, \tag{2.13}$$

with some ℓ-independent efficiency constant $C_{\rm eff} > 0$ and reliability constant $C_{\rm rel} > 0$. In the definition of $\mu_\ell^\star$, $(\cdot)'$ denotes the arclength derivative, and $h_\ell \in L^\infty(\Gamma)$ denotes the local mesh-size which is defined elementwise by $h_\ell|_E := \operatorname{diam}(E)$ for $E \in \mathcal{E}_\ell$. Moreover, we define the data oscillations by

$$\operatorname{osc}_\ell := \big(\|h_\ell^{1/2}(u_D - I_\ell u_D)'\|_{L^2(\Gamma_D)}^2 + \|h_\ell^{1/2}(\phi_N - \Pi_\ell \phi_N)\|_{L^2(\Gamma_N)}^2\big)^{1/2}. \tag{2.14}$$

Under the saturation assumption (2.11) and with the perturbed error estimator

$$\mu_\ell := \big(\|h_\ell^{1/2}(\widehat{U}_{N,\ell} - I_\ell \widehat{U}_{N,\ell})'\|_{L^2(\Gamma_N)}^2 + \|h_\ell^{1/2}(\widehat{\Phi}_{D,\ell} - \Pi_\ell \widehat{\Phi}_{D,\ell})\|_{L^2(\Gamma_D)}^2\big)^{1/2}, \tag{2.15}$$

Theorem 4.2 proves an upper bound for the perturbed Galerkin error

$$C_{\rm rel}^{-1}\, |||\mathbf{u} - \mathbf{U}_\ell||| \le \varrho_\ell := (\mu_\ell^2 + \operatorname{osc}_\ell^2)^{1/2} \tag{2.16}$$

as well as a lower bound

$$C_{\rm eff}^{-1}\, \varrho_\ell \le |||\mathbf{u} - \mathbf{U}_\ell||| + \operatorname{osc}_\ell \tag{2.17}$$

up to data oscillations.

2.4. Adaptive mesh-refining algorithm. In Section 5, we introduce an adaptive mesh-refining algorithm which is steered by the local contributions of the estimator ϱ_ℓ (Algorithm 5.1) defined in (2.16). This provides a sequence of nested spaces $\mathcal{X}_\ell \subset \mathcal{X}_{\ell+1}$, corresponding Galerkin solutions $\mathbf{U}_\ell \in \mathcal{X}_\ell$, and error estimators ϱ_ℓ. Theorem 5.4 guarantees that, independent of the saturation assumption (2.11), the adaptive algorithms leads to

$$\lim_{\ell\to\infty} \mu_\ell = 0 = \lim_{\ell\to\infty} \operatorname{osc}_\ell. \tag{2.18}$$

According to (2.16), the saturation assumption (2.11) for the non-perturbed problem thus yields convergence of the discrete Galerkin solutions $\mathbf{U}_\ell \in \mathcal{X}_\ell$ to the exact solution $\mathbf{u} \in \mathcal{H}$.

Our proof of (2.18) relies on the concept of *estimator reduction* introduced in [3]: First, we observe that the proposed Galerkin scheme guarantees some a priori convergence $\lim_\ell \widehat{\mathbf{U}}_\ell = \widehat{\mathbf{u}}_\infty$ towards some limit $\widehat{\mathbf{u}}_\infty \in \mathcal{H}$ (Proposition 5.2). Second, we prove that the estimator ϱ_ℓ satisfies

$$\varrho_{\ell+1}^2 \le q\, \varrho_\ell^2 + C\, |||\widehat{\mathbf{U}}_{\ell+1} - \widehat{\mathbf{U}}_\ell|||^2 \quad \text{for all } \ell \in \mathbb{N}_0 \tag{2.19}$$

with some ℓ-independent constants $0 < q < 1$ and $C > 0$. Together with the a priori convergence, elementary calculus thus proves $\lim_\ell \varrho_\ell = 0$.

2.5. Inclusion of non-homogeneous volume forces. In Section 6, we extend the developed ideas to the case of a non-homogeneous volume force $f \in \widetilde{H}^{-1}(\Omega)$, i.e.,

$$-\Delta u = f \quad \text{in } \Omega. \tag{2.20}$$

In the boundary integral formulation (2.2), the right-hand side then additionally involves the trace $N_0 f$ and the normal derivative $N_1 f$ of the Newtonian potential. Under additional regularity $f \in L^2(\Omega)$, we replace the volume force f by a certain L^2-projection f_ℓ with respect to a volume partition $\mathcal{T}_\ell$. Moreover, to avoid the implementation of $N_1 f_\ell$, it is approximated by use of $N_0 f_\ell$ and an additional integral formulation, cf. Section 6.2 below. Theorem 6.1 includes these additional consistency errors into the a posteriori error estimate. Under an appropriate saturation assumption, we provide a computable upper bound ϱ_ℓ for the error. We propose an adaptive mesh-refinement which steers both, the refinement of the boundary mesh as well as the resolution of the volume data (Algorithm 6.2). In analogy to the case $f = 0$, Theorem 6.3 proves that the adaptive algorithm drives the underlying error estimator ϱ_ℓ to zero.

3. Preliminaries

In this section, we recall the definition of the involved fractional-order Sobolev spaces on the boundary as well as the involved boundary integral operators and their properties. For proofs, the reader is referred to the monographs [25, 29, 30]. Finally, this section collects our notation for the boundary discretization as well as the approximation estimates and inverse estimates used below.

3.1. Sobolev spaces on the boundary. For $\omega \subset \Omega$, the usual Sobolev spaces are denoted by $L^2(\omega)$ and $H^1(\omega)$. We define the Sobolev Spaces on the boundary as the space of traces, i.e.,

$$H^{1/2}(\Gamma) := \big\{ u|_\Gamma \mid u \in H^1(\Omega) \big\}.$$

For relatively open subsets $\gamma \subset \Gamma$, we define the space $H^{1/2}(\gamma)$ as the space of restrictions of functions in $H^{1/2}(\Gamma)$, and $\widetilde{H}^{1/2}(\gamma) \subset H^{1/2}(\gamma)$ is the space of functions which can be extended by zero to $H^{1/2}(\Gamma)$. The dual space of $H^{1/2}(\gamma)$ is denoted by $\widetilde{H}^{-1/2}(\gamma)$, whereas the dual space of $\widetilde{H}^{1/2}(\gamma)$ is denoted by $H^{-1/2}(\gamma)$. In both cases, duality is understood via the extended L^2-scalar product.

3.2. Weakly-singular integral operator. The simple-layer potential

$$V\phi(x) := -\frac{1}{2\pi} \int_\gamma \log|x-y|\, \phi(y)\, ds_y \quad \text{for } x \in \Gamma \tag{3.1}$$

defines a continuous and symmetric linear operator $V \in L(\widetilde{H}^{-1/2}(\gamma), H^{1/2}(\gamma))$, for a relatively open arc $\gamma \subseteq \Gamma = \partial\Omega$. Provided that $\operatorname{diam}(\Omega) < 1$, V is elliptic. Therefore, $(\phi, \psi)_{V(\gamma)} := \langle V\phi, \psi \rangle$ defines a scalar product on $\widetilde{H}^{-1/2}(\gamma)$, and the induced norm $\|\phi\|_{V(\gamma)} := (\phi, \phi)_{V(\gamma)}^{1/2}$ is an equivalent norm on $\widetilde{H}^{-1/2}(\gamma)$.

3.3. Hypersingular integral operator. Let $\gamma \subset \Gamma$ be a relatively open arc with $\overline{\gamma} \subsetneq \Gamma$. The hypersingular integral operator is formally defined by

$$Wu(x) := \frac{1}{2\pi} \partial_{n(x)} \int_\gamma \partial_{n(y)} \log|x-y|\, u(y)\, ds_y \quad \text{for } x \in \Gamma. \tag{3.2}$$

It can be understood through Nédeléc's formula

$$\langle Wu\,,v\rangle = \langle Vu'\,,v'\rangle \quad \text{for all } u,v\in H^1(\Gamma), \tag{3.3}$$

which provides a link between W and the simple-layer potential V. Then, W defines a continuous, symmetric, and elliptic linear operator $W \in L(\widetilde{H}^{1/2}(\gamma), H^{-1/2}(\gamma))$. In particular, $(u\,,v)_{W(\gamma)} := \langle Wu\,,v\rangle$ defines a scalar product on $\widetilde{H}^{1/2}(\gamma)$, and the induced norm $\|u\|_{W(\gamma)} := (u\,,u)^{1/2}_{W(\gamma)}$ is an equivalent norm on $\widetilde{H}^{1/2}(\gamma)$.

3.4. Calderón projector *A*. Besides the simple-layer potential V and the hypersingular integral operator W, the definition of the Calderón projector A in (2.2) involves the double-layer potential $K \in L(H^{1/2}(\Gamma), H^{1/2}(\Gamma))$ formally defined by

$$Ku(x) := -\frac{1}{2\pi}\int_\gamma \partial_{n(y)} \log|x-y|\, u(y)\, ds_y \quad \text{for } x\in\Gamma, \tag{3.4}$$

and its adjoint $K' \in L(H^{-1/2}(\Gamma), H^{-1/2}(\Gamma))$, i.e. there holds

$$\langle K'\phi\,,u\rangle = \langle \phi\,, Ku\rangle \quad \text{for all } \phi\in H^{-1/2}(\Gamma) \text{ and } u\in H^{1/2}(\Gamma). \tag{3.5}$$

The non-symmetric bilinear form $\langle\!\langle \cdot\,,\cdot\rangle\!\rangle$ from (2.4) thus satisfies

$$|||(u,\phi)|||^2 := \langle\!\langle (u,\phi)\,,(u,\phi)\rangle\!\rangle = \langle V\phi\,,\phi\rangle + \langle Wu\,,u\rangle = \|\phi\|^2_{V(\Gamma_D)} + \|u\|^2_{W(\Gamma_N)}. \tag{3.6}$$

Recall that we assume $\operatorname{diam}(\Omega) < 1$. Since $\|\cdot\|_{W(\Gamma_N)}$ is an equivalent norm on $\widetilde{H}^{1/2}(\Gamma_N)$ and $\|\cdot\|_{V(\Gamma_D)}$ is an equivalent norm on $\widetilde{H}^{-1/2}(\Gamma_D)$, the energy norm $|||\cdot|||$ defines an equivalent norm on the energy space $\mathcal{H} = \widetilde{H}^{1/2}(\Gamma_N)\times\widetilde{H}^{-1/2}(\Gamma_D)$.

The relation between (2.1) and (2.2) reads as follows: If $\widetilde{u}\in H^1(\Omega)$ is the solution of (2.1), we define $u := \widetilde{u}|_\Gamma \in H^{1/2}(\Gamma)$ and $\phi := \partial_n\widetilde{u}|_\Gamma \in H^{-1/2}(\Gamma)$. If $(u_D,\phi_N)\in H^{1/2}(\Gamma)\times H^{-1/2}(\Gamma)$ are arbitrary extensions of the given Dirichlet and Neumann data, $(u_N,\phi_D) := (u-u_D, \phi-\phi_N)$ satisfies $(u_N,\phi_D)\in\mathcal{H}$ and solves (2.5). Conversely, let $(u_N,\phi_D)\in\mathcal{H}$ be the unique solution of (2.5). Extending (u_N,ϕ_D) by zero, we obtain $(u_N,\phi_D)\in H^{1/2}(\Gamma)\times H^{-1/2}(\Gamma)$. Defining $(u,\phi) := (u_D+u_N, \phi_D+\phi_N)$, the solution of (2.1) is given by the representation formula

$$\widetilde{u} = V\phi - Ku \quad \text{in } \Omega, \tag{3.7}$$

where the integrals $V\phi$ and Ku are now evaluated for $x\in\Omega$ instead of $x\in\Gamma$.

3.5. Boundary discretization. Let $\mathcal{E}_\ell = \{E_1,\dots,E_N\}$ be a finite partition of Γ into non-degenerate boundary pieces. For simplicity, we assume that the elements $E\in\mathcal{E}_\ell$ are affine line segments. We define the local mesh-width $h_\ell\in L^\infty(\Gamma)$ by $h_\ell|_E := \operatorname{diam}(E) > 0$ for $E\in\mathcal{E}_\ell$. We assume that $\mathcal{E}_\ell$ resolves the boundary conditions in the sense that each element $E\in\mathcal{E}_\ell$ satisfies either $E\subseteq\overline{\Gamma}_D$ or $E\subseteq\overline{\Gamma}_N$. For $\gamma\in\{\Gamma_D,\Gamma_N\}$, we then define the restricted meshes $\mathcal{E}_\ell|_\gamma := \{E_j\in\mathcal{E}_\ell \mid E_j\subseteq\bar\gamma\}$.

Let $\mathcal{P}^p(\mathcal{E}_\ell|_\gamma)$ be the space of $\mathcal{E}_\ell|_\gamma$-piecewise polynomials of degree p with respect to the arclength. Then, $\mathcal{S}^1(\mathcal{E}_\ell|_\gamma) := \mathcal{P}^1(\mathcal{E}_\ell|_\gamma)\cap C(\gamma)$ is the space of piecewise affine and globally continuous functions, and $\mathcal{S}^1_0(\mathcal{E}_\ell|_\gamma) := \{u\in\mathcal{S}^1(\mathcal{E}_\ell|_\gamma)\mid u|_{\partial\gamma}=0\}$.

Refinement of an element $E\in\mathcal{E}_\ell$ is done by bisection, i.e. E is split into two sons $E_1,E_2\in\mathcal{E}_{\ell+1}$ with $h_{\ell+1}|_{E_j} = h_\ell|_E/2$, for $j=1,2$. Crucial estimates in the analysis depend on an upper bound for the K-mesh constant, which is defined by

$$\kappa(\mathcal{E}_\ell) := \max\left\{h_\ell|_E/h_\ell|_{E'} \mid E,E'\in\mathcal{E}_\ell \text{ are neighbours }\right\}.$$

In particular, we use a local mesh-refinement strategy which guarantees

$$\sup_{\ell\in\mathbb{N}} \kappa(\mathcal{E}_\ell) \le 2\kappa(\mathcal{E}_0)$$

where $\mathcal{E}_0$ is the initial partition for the adaptive algorithm, see [4, Section 2].

3.6. Inverse estimates. Let $\gamma \in \{\Gamma_D, \Gamma_N\}$. According to [19, Theorem 3.6] there holds the inverse estimate

$$\|h_\ell^{1/2}\Psi_\ell\|_{L^2(\gamma)} \le c_{\rm inv}\,\|\Psi_\ell\|_{\widetilde{H}^{-1/2}(\gamma)} \quad \text{for all } \Psi_\ell \in \mathcal{P}^0(\mathcal{E}_\ell|_\gamma), \tag{3.8}$$

where the constant $c_{\rm inv} > 0$ depends only on γ and an upper bound of the local mesh ratio $\kappa(\mathcal{E}_\ell|_\gamma) \le \kappa(\mathcal{E}_\ell)$. According to [9, Proposition 3.1], there holds the inverse estimate

$$\|h_\ell^{1/2}V_\ell'\|_{L^2(\gamma)} \le C_{\rm inv}\,\|V_\ell\|_{\widetilde{H}^{1/2}(\gamma)} \quad \text{for all } V_\ell \in \mathcal{S}^1_0(\mathcal{E}_\ell|_\gamma), \tag{3.9}$$

where $C_{\rm inv} > 0$ depends only on $\gamma \subsetneqq \Gamma$.

3.7. Approximation estimates. Let $\gamma \in \{\Gamma_D, \Gamma_N\}$ and let $\Pi_\ell : L^2(\gamma) \to \mathcal{P}^0(\mathcal{E}_\ell|_\gamma)$ denote the L^2-orthogonal projection onto $\mathcal{P}^0(\mathcal{E}_\ell|_\gamma)$. According to [8, Theorem 4.1] there holds

$$c_{\rm apx}^{-1}\,\|\phi - \Pi_\ell\phi\|_{\widetilde{H}^{-1/2}(\gamma)} \le \|h_\ell^{1/2}(\phi - \Pi_\ell\phi)\|_{L^2(\gamma)} \le \|h_\ell^{1/2}\phi\|_{L^2(\gamma)} \quad \text{for all } \phi \in L^2(\gamma), \tag{3.10}$$

where the constant $c_{\rm apx} > 0$ depends only on γ, see also [15, Lemma 2.1]. Recall that the Sobolev inequality yields $H^1(\gamma) \subset \mathcal{C}(\overline{\gamma})$ so that nodal interpolation

$$I_\ell u := \sum_{z\in\mathcal{K}_\ell} u(z)\varphi_z \in \mathcal{S}^1_0(\mathcal{E}_\ell|_\gamma), \tag{3.11}$$

with $\mathcal{K}_\ell$ the set of nodes of the triangulation $\mathcal{E}_\ell$, is well-defined for $u \in H^1(\gamma)$. According to [7, Theorem 1], there holds the approximation result

$$\|u - I_\ell u\|_{\widetilde{H}^{1/2}(\gamma)} \le C_{\rm apx}\,\|h_\ell^{1/2}u'\|_{L^2(\gamma)} \quad \text{for all } u \in H^1(\gamma)\cap\widetilde{H}^{1/2}(\gamma), \tag{3.12}$$

where the constant $C_{\rm apx} > 0$ depends only on γ and an upper bound of the local mesh-ratio $\kappa(\mathcal{E}_\ell|_\gamma) \le \kappa(\mathcal{E}_\ell)$. Simple post-processing [16, Lemma 2.2] reveals

$$C_{\rm apx}^{-1}\,\|u - I_\ell u\|_{\widetilde{H}^{1/2}(\gamma)} \le \|h_\ell^{1/2}(u - I_\ell u)'\|_{L^2(\gamma)} \le \|h_\ell^{1/2}u'\|_{L^2(\gamma)} \quad \text{for all } u \in H^1(\gamma)\cap\widetilde{H}^{1/2}(\gamma) \tag{3.13}$$

even with the same constant $C_{\rm apx} > 0$. We stress the well-known identity $(I_\ell u)' = \Pi_\ell u'$ in 1D, which will be used lateron.

4. A posteriori error estimation

Note that the solution $\mathbf{u} = (u_N, \phi_D) \in \mathcal{H}$ of (2.2) clearly depends on the extension of the given boundary data $(u_D, \phi_N) \in H^{1/2}(\Gamma_D) \times H^{-1/2}(\Gamma_N)$ to a couple $(u_D, \phi_N) \in H^{1/2}(\Gamma) \times H^{-1/2}(\Gamma)$. To fix particular extensions, recall the additional regularity assumption $(u_D, \phi_N) \in H^1(\Gamma_D) \times L^2(\Gamma_N)$.

We extend ϕ_N by zero from Γ_N to $\phi_N \in L^2(\Gamma)$. For the extension of u_D, note that the Sobolev inequality provides $H^1(\Gamma_D) \subset \mathcal{C}(\overline{\Gamma}_D)$. Since Γ_D and Γ_N are resolved by the initial boundary partition $\mathcal{E}_0$, we find a continuous extension $u_D : \Gamma \to \mathbb{R}$ such that $u_D|_{\Gamma_N}$ is $\mathcal{E}_0$-piecewise affine. In particular, this extension satisfies $u_D \in H^1(\Gamma)$.

Let $\mathcal{E}_\ell$ be a certain refinement of $\mathcal{E}_0$. In particular, $\mathcal{E}_\ell$ resolves the boundary conditions and $u_D|_{\Gamma_N}$ is $\mathcal{E}_\ell$-piecewise affine. To keep the presentation short, we use the abbreviate notation from Section 2. We just recall that $\mathbf{U}_\ell^\star \in \mathcal{X}_\ell$ and $\widehat{\mathbf{U}}_\ell^\star \in \widehat{\mathcal{X}}_\ell$ are the Galerkin

solutions (2.7) with respect to the exact right-hand side F, whereas the Galerkin solutions (2.10) with respect to the perturbed right-hand side F_ℓ are denoted by $\mathbf{U}_\ell \in \mathcal{X}_\ell$ and $\widehat{\mathbf{U}}_\ell \in \widehat{\mathcal{X}}_\ell$.

Theorem 4.1. *There is a constant $C_1 > 0$ which depends only on Γ_D, Γ_N, and $\kappa(\mathcal{E}_\ell)$ such that*

$$\mu_\ell^\star \le C_1 \, |||\mathbf{u} - \mathbf{U}_\ell^\star|||. \tag{4.1}$$

Under the saturation assumption (2.11)*, there holds*

$$|||\mathbf{u} - \mathbf{U}_\ell^\star||| \le C_2 \, \mu_\ell^\star, \tag{4.2}$$

where the constant $C_2 > 0$ depends only on Γ_D, Γ_N, $\kappa(\mathcal{E}_\ell)$, and $C_{\rm sat} \in (0,1)$.

Proof. The proof follows along the lines of [18, 15, 16] and is thus only sketched for the convenience of the reader. We first prove that $\mu_\ell^\star$ is equivalent to the canonical $(h-h/2)$-error estimator $\eta_\ell^\star := |||\widehat{\mathbf{U}}_\ell^\star - \mathbf{U}_\ell^\star|||$. To see this, we recall that $\mathbf{U}_\ell^\star \in \mathcal{X}_\ell$ is also the Galerkin approximation of $\widehat{\mathbf{U}}_\ell^\star$. Moreover, Galerkin solutions are quasi-optimal, i.e., there holds

$$\begin{aligned}\eta_\ell^\star = |||\widehat{\mathbf{U}}_\ell^\star - \mathbf{U}_\ell^\star||| \lesssim \min_{\mathbf{V}_\ell \in \mathcal{X}_\ell} |||\widehat{\mathbf{U}}_\ell^\star - \mathbf{V}_\ell||| &\le |||\widehat{\mathbf{U}}_\ell^\star - (I_\ell \widehat{U}_{N,\ell}^\star, \Pi_\ell \widehat{\Phi}_{D,\ell}^\star)||| \\ &= \big(\|\widehat{U}_{N,\ell}^\star - I_\ell \widehat{U}_{N,\ell}^\star\|_{W(\Gamma_N)}^2 + \|\widehat{\Phi}_{D,\ell}^\star - \Pi_\ell \widehat{\Phi}_{D,\ell}^\star\|_{V(\Gamma_D)}^2\big)^{1/2}.\end{aligned}$$

Now, we use norm equivalences $\|\cdot\|_{V(\Gamma_D)} \sim \|\cdot\|_{\widetilde{H}^{-1/2}(\Gamma_D)}$ and $\|\cdot\|_{W(\Gamma_N)} \sim \|\cdot\|_{\widetilde{H}^{1/2}(\Gamma_N)}$ as well as the approximation estimates (3.10) and (3.13) to see

$$\big(\|\widehat{U}_{N,\ell}^\star - I_\ell \widehat{U}_{N,\ell}^\star\|_{W(\Gamma_N)}^2 + \|\widehat{\Phi}_{D,\ell}^\star - \Pi_\ell \widehat{\Phi}_{D,\ell}^\star\|_{V(\Gamma_D)}^2\big)^{1/2} \lesssim \mu_\ell^\star.$$

This proves $\eta_\ell^\star \lesssim \mu_\ell^\star$. To see the converse inequality, recall that the L^2-projection onto $\mathcal{P}^0(\mathcal{E}_\ell)$ is even the $\mathcal{E}_\ell$-piecewise best approximation operator, i.e.

$$\|\widehat{\Phi}_{D,\ell}^\star - \Pi_\ell \widehat{\Phi}_{D,\ell}^\star\|_{L^2(E)} = \min_{c \in \mathbb{R}} \|\widehat{\Phi}_{D,\ell}^\star - c\|_{L^2(E)} \le \|\widehat{\Phi}_{D,\ell}^\star - \Phi_{D,\ell}^\star\|_{L^2(E)} \text{ for all } E \in \mathcal{E}_\ell \text{ with } E \subseteq \overline{\Gamma}_D.$$

Together with the identity $(I_\ell u)' = \Pi_\ell u'$, the same argument proves

$$\|(\widehat{U}_{N,\ell}^\star - I_\ell \widehat{U}_{N,\ell}^\star)'\|_{L^2(E)} \le \|(\widehat{U}_{N,\ell}^\star - U_{N,\ell}^\star)'\|_{L^2(E)} \quad \text{for all } E \in \mathcal{E}_\ell \text{ with } E \subseteq \overline{\Gamma}_N.$$

The $h_\ell^{1/2}$-weighted ℓ_2-sum of the last two estimates now yields

$$\mu_\ell^\star \le \big(\|h_\ell^{1/2}(\widehat{U}_{N,\ell}^\star - U_{N,\ell}^\star)'\|_{L^2(\Gamma_N)}^2 + \|h_\ell^{1/2}(\widehat{\Phi}_{D,\ell}^\star - \Phi_{D,\ell}^\star)\|_{L^2(\Gamma_D)}^2\big)^{1/2} \lesssim \eta_\ell^\star,$$

where we have finally used the inverse estimates (3.8)–(3.9). Therefore, it only remains to prove that (4.1)–(4.2) hold with $\mu_\ell^\star$ replaced by $\eta_\ell^\star$. To see the lower bound, note that Galerkin orthogonality and continuity of $\langle\!\langle \cdot, \cdot \rangle\!\rangle$ yield

$$\begin{aligned}(\eta_\ell^\star)^2 = \langle\!\langle \widehat{\mathbf{U}}_\ell^\star - \mathbf{U}_\ell^\star, \widehat{\mathbf{U}}_\ell^\star - \mathbf{U}_\ell^\star \rangle\!\rangle = \langle\!\langle \mathbf{u} - \mathbf{U}_\ell^\star, \widehat{\mathbf{U}}_\ell^\star - \mathbf{U}_\ell^\star \rangle\!\rangle &\lesssim |||\mathbf{u} - \mathbf{U}_\ell^\star||| \, |||\widehat{\mathbf{U}}_\ell^\star - \mathbf{U}_\ell^\star||| \\ &= |||\mathbf{u} - \mathbf{U}_\ell^\star||| \, \eta_\ell^\star.\end{aligned}$$

The upper bound follows from

$$|||\mathbf{u} - \mathbf{U}_\ell^\star||| \le |||\mathbf{u} - \widehat{\mathbf{U}}_\ell^\star||| + |||\widehat{\mathbf{U}}_\ell^\star - \mathbf{U}_\ell^\star||| = |||\mathbf{u} - \widehat{\mathbf{U}}_\ell^\star||| + \eta_\ell^\star \le C_{\rm sat} \, |||\mathbf{u} - \mathbf{U}_\ell^\star||| + \eta_\ell^\star,$$

which results in $|||\mathbf{u} - \mathbf{U}_\ell^\star||| \le (1 - C_{\rm sat})^{-1} \, \eta_\ell^\star$. □

Theorem 4.2. *There is a constant $C_3 > 1$ which only depends on Γ_D, Γ_N, and $\kappa(\mathcal{E}_\ell)$ such that*

$$\mu_\ell \le \mu_\ell^\star + C_3 \operatorname{osc}_\ell \quad \text{as well as} \quad \mu_\ell^\star \le \mu_\ell + C_3 \operatorname{osc}_\ell \le \sqrt{2}\, C_3\, \varrho_\ell \tag{4.3}$$

with $\varrho_\ell = (\mu_\ell^2 + \operatorname{osc}_\ell^2)^{1/2}$. Moreover, there holds

$$|||\mathbf{U}_\ell^\star - \mathbf{U}_\ell||| \le C_3 \operatorname{osc}_\ell. \tag{4.4}$$

In particular, this yields

$$C_4^{-1}\, \varrho_\ell \le |||\mathbf{u} - \mathbf{U}_\ell||| + \operatorname{osc}_\ell, \tag{4.5}$$

where the constant $C_4 > 0$ depends only on Γ_D, Γ_N, and $\kappa(\mathcal{E}_\ell)$. Under the saturation assumption (2.11) *for the non-perturbed problem, there holds*

$$|||\mathbf{u} - \mathbf{U}_\ell||| \le C_5\, \varrho_\ell. \tag{4.6}$$

where the constant $C_5 > 0$ additionally depends on the saturation constant $C_{\rm sat} \in (0,1)$.

Proof. Triangle inequality and $\mathcal{E}_\ell$-piecewise L^2-orthogonality yield

$$\begin{aligned}\mu_\ell &\le \mu_\ell^\star + \big(\|h_\ell^{1/2}[(1-I_\ell)(\widehat{U}_{N,\ell}^\star - \widehat{U}_{N,\ell})]'\|_{L^2(\Gamma_N)}^2 + \|h_\ell^{1/2}(1-\Pi_\ell)(\widehat{\Phi}_{D,\ell}^\star - \widehat{\Phi}_{D,\ell})\|_{L^2(\Gamma_D)}^2\big)^{1/2}\\ &\le \mu_\ell^\star + \big(\|h_\ell^{1/2}(\widehat{U}_{N,\ell}^\star - \widehat{U}_{N,\ell})'\|_{L^2(\Gamma_N)}^2 + \|h_\ell^{1/2}(\widehat{\Phi}_{D,\ell}^\star - \widehat{\Phi}_{D,\ell})\|_{L^2(\Gamma_D)}^2\big)^{1/2}.\end{aligned}$$

The inverse estimates (3.8)–(3.9) and equivalence of norms conclude

$$\mu_\ell \le \mu_\ell^\star + C\,\big(\|\widehat{U}_{N,\ell}^\star - \widehat{U}_{N,\ell}\|_{W(\Gamma_N)}^2 + \|\widehat{\Phi}_{D,\ell}^\star - \widehat{\Phi}_{D,\ell}\|_{V(\Gamma_D)}^2\big)^{1/2} = \mu_\ell^\star + C\,|||\widehat{\mathbf{U}}_\ell^\star - \widehat{\mathbf{U}}_\ell|||.$$

Since the Galerkin solutions depend linearly and continuously on the data, the mapping properties of the involved boundary integral operators yield

$$|||\widehat{\mathbf{U}}_\ell^\star - \widehat{\mathbf{U}}_\ell||| \lesssim \|u_D - I_\ell u_D\|_{H^{1/2}(\Gamma)} + \|\phi_N - \Pi_\ell \phi_N\|_{H^{-1/2}(\Gamma)}.$$

Now, we may apply the approximation estimates (3.10) and (3.13) to see

$$|||\widehat{\mathbf{U}}_\ell^\star - \widehat{\mathbf{U}}_\ell||| \lesssim \|h_\ell^{1/2}(u_D - I_\ell u_D)'\|_{L^2(\Gamma)} + \|h_\ell^{1/2}(\phi_N - \Pi_\ell\phi_N)\|_{L^2(\Gamma)} \lesssim \operatorname{osc}_\ell.$$

Here, we have finally used that ϕ_N is identified with its trivial extension $\phi_N \in L^2(\Gamma)$, i.e. $\phi_N|_{\Gamma_D} = 0$ and that u_D is extended linearly to $u_D \in H^1(\Gamma)$, i.e. $u_D|_{\Gamma_N} = I_0 u_D|_{\Gamma_N} = I_\ell u_D|_{\Gamma_N}$, where I_0 denotes nodal interpolation with respect to the initial mesh $\mathcal{E}_0$. This proves the first estimate in (4.3), and the second follows by the same arguments. The estimate $|||\mathbf{U}_\ell^\star - \mathbf{U}_\ell||| \lesssim \operatorname{osc}_\ell$ follows as before.

To prove the efficiency estimate (4.5), we use (4.1) as well as (4.3) to see

$$\begin{aligned}\varrho_\ell \lesssim \mu_\ell + \operatorname{osc}_\ell \lesssim \mu_\ell^\star + \operatorname{osc}_\ell \lesssim |||\mathbf{u} - \mathbf{U}_\ell^\star||| + \operatorname{osc}_\ell &\le |||\mathbf{u} - \mathbf{U}_\ell||| + |||\mathbf{U}_\ell^\star - \mathbf{U}_\ell||| + \operatorname{osc}_\ell\\ &\lesssim |||\mathbf{u} - \mathbf{U}_\ell||| + \operatorname{osc}_\ell.\end{aligned}$$

The reliability estimate (4.6) follows from

$$|||\mathbf{u} - \mathbf{U}_\ell||| \le |||\mathbf{u} - \mathbf{U}_\ell^\star||| + |||\mathbf{U}_\ell^\star - \mathbf{U}_\ell||| \lesssim \mu_\ell^\star + \operatorname{osc}_\ell \lesssim \mu_\ell + \operatorname{osc}_\ell \lesssim \varrho_\ell.$$

This concludes the proof. □

5. Adaptive mesh-refining algorithm

The adaptive mesh-refinement introduced subsequently is steered by the refinement indicators

$$\varrho_\ell(E)^2 := \begin{cases} \|h_\ell^{1/2}(\widehat{U}_{N,\ell} - I_\ell \widehat{U}_{N,\ell})'\|^2_{L^2(E)} + \|h_\ell^{1/2}(\phi_N - \Pi_\ell \phi_N)\|^2_{L^2(E)} & \text{for } E \subseteq \Gamma_N, \\ \|h_\ell^{1/2}(\widehat{\Phi}_{D,\ell} - \Pi_\ell \widehat{\Phi}_{D,\ell})\|^2_{L^2(E)} + \|h_\ell^{1/2}(u_D - I_\ell u_D)'\|^2_{L^2(E)} & \text{for } E \subseteq \Gamma_D, \end{cases} \tag{5.1}$$

defined for all $E \in \mathcal{E}_\ell$. Note that

$$\varrho_\ell^2 = \sum_{E \in \mathcal{E}_\ell} \varrho_\ell(E)^2 = \mu_\ell^2 + \operatorname{osc}_\ell^2. \tag{5.2}$$

These indicators are used to mark certain elements $\mathcal{M}_\ell \subseteq \mathcal{E}_\ell$ for refinement. Based on some fixed parameter $\theta \in (0,1]$, the set $\mathcal{M}_\ell$ of marked elements is determined by use of the Dörfler marking (5.3) introduced in [14].

Algorithm 5.1. Input*: Initial partition $\mathcal{E}_0$, parameter $\theta \in (0,1]$, counter $\ell := 0$.*

(i) *Construct uniform refinement $\widehat{\mathcal{E}}_\ell$ of $\mathcal{E}_\ell$.*
(ii) *Compute Galerkin solution $\widehat{\mathbf{U}}_\ell = (\widehat{U}_{N,\ell}, \widehat{\Phi}_{D,\ell}) \in \widehat{\mathcal{X}}_\ell := \mathcal{S}^1_0(\widehat{\mathcal{E}}_\ell|_{\Gamma_N}) \times \mathcal{P}^0(\widehat{\mathcal{E}}_\ell|_{\Gamma_D})$.*
(iii) *Compute refinement indicators $\varrho_\ell(E)$ for all $E \in \mathcal{E}_\ell$.*
(iv) *Determine minimal set $\mathcal{M}_\ell \subseteq \mathcal{E}_\ell$ such that*

$$\theta\, \varrho_\ell^2 \le \sum_{E \in \mathcal{M}_\ell} \varrho_\ell(E)^2. \tag{5.3}$$

(v) *Refine at least all marked elements $\mathcal{M}_\ell$ to obtain a mesh $\mathcal{E}_{\ell+1}$ with $\kappa(\mathcal{E}_{\ell+1}) \le 2\,\kappa(\mathcal{E}_0)$.*
(vi) *Increase counter $\ell \mapsto \ell + 1$ and go to* (i).

Output*: Sequences of meshes $\mathcal{E}_\ell$, discrete solutions $\widehat{\mathbf{U}}_\ell$, and error estimators $\varrho_\ell = (\mu_\ell^2 + \operatorname{osc}_\ell^2)^{1/2}$.* □

Remark 1. *Algorithm 5.1 is formulated in the usual form*

$$\boxed{Solve} \mapsto \boxed{Estimate} \mapsto \boxed{Mark} \mapsto \boxed{Refine.}$$

However, note that the Galerkin solution $\mathbf{U}_\ell \in \mathcal{X}_\ell$ which is controlled in terms of the error estimator ϱ_ℓ is not computed throughout. Instead, we only compute the improved Galerkin solution $\widehat{\mathbf{U}}_\ell \in \widehat{\mathcal{X}}_\ell$ with respect to a uniformly refined mesh. From that point of view, our adaptive algorithm can be understood in the form

$$\boxed{RefineUniformly} \mapsto \boxed{Solve} \mapsto \boxed{Estimate} \mapsto \boxed{Mark} \mapsto \boxed{Coarsen.}$$

Moreover, to compute $\widehat{\mathbf{U}}_\ell$, the operators V, K, and W are discretized with respect to $\widehat{\mathcal{E}}_\ell$ on the left-hand side of (2.10)*. It is therefore obvious to use the improved data approximation $\widehat{I}_\ell u_D$ and $\widehat{\Pi}_\ell \phi_N$ even on the right-hand side* (2.9)–(2.10)*. Note that this only leads to minor modifications of osc_ℓ, whereas the a posteriori analysis of Section 4 is not affected.* □

Remark 2. *For the local mesh-refinement in step (v) of Algorithm 5.1, we use the algorithm proposed in* [4, Section 2.2]*. This is proven to guarantee boundedness $\kappa(\mathcal{E}_\ell) \le 2\,\kappa(\mathcal{E}_0)$, while still being optimal in the sense that*

$$\#\mathcal{E}_\ell - \#\mathcal{E}_0 \lesssim \sum_{j=0}^{\ell-1} \#\mathcal{M}_j,$$

i.e., the number of elements in $\mathcal{E}_\ell$ is essentially given by the number of elements which have been refined in the previous steps of Algorithm 5.1. □

Before we prove convergence of Algorithm 5.1 in Theorem 5.4 below, we first state that there holds a priori convergence, i.e., the sequence $\mathbf{U}_\ell$ of discrete solutions always tends to some limit $\mathbf{u}_\infty$.

Proposition 5.2. *Let $\mathcal{E}_\ell$ be a sequence of meshes with corresponding nested spaces $\mathcal{X}_\ell$, i.e., $\mathcal{X}_\ell \subseteq \mathcal{X}_{\ell+1}$ for all $\ell \in \mathbb{N}_0$. Let $\mathbf{U}_\ell^\star$ and $\mathbf{U}_\ell$ be the corresponding Galerkin solutions of (2.7) and (2.10), respectively. Then, there are a priori limits $\mathbf{u}_\infty^\star, \mathbf{u}_\infty \in \mathcal{H}$ such that*

$$\lim_{\ell\to\infty} |||\mathbf{u}_\infty^\star - \mathbf{U}_\ell^\star||| = 0 = \lim_{\ell\to\infty} |||\mathbf{u}_\infty - \mathbf{U}_\ell|||. \tag{5.4}$$

The proof needs the following elementary result, which is found in e.g. [3, 11, 26].

Lemma 5.3. *Let H be a Hilbert space and $X_\ell \subset X_{\ell+1}$ be a sequence of nested closed subspaces of H. Let $\mathbb{P}_\ell : H \to X_\ell$ be the orthogonal projection onto X_ℓ and $x \in H$. Then, the limit $x_\infty := \lim_\ell \mathbb{P}_\ell x \in H$ exists and belongs to the closure of $X_\infty := \bigcup_{\ell=0}^\infty X_\ell$ with respect to H.* □

Proof of a priori convergence of $\mathbf{U}_\ell^\star$. Applying Lemma 5.3 to $H = \mathcal{H}$, $X_\ell = \mathcal{X}_\ell$, and the exact solution $\mathbf{u} \in \mathcal{H}$, we see that the limit $\mathbf{u}_\infty^\star := \lim_\ell \mathbb{P}_\ell \mathbf{u}$ exists and belongs to the closure of $\mathcal{X}_\infty := \bigcup_{\ell=0}^\infty \mathcal{X}_\ell$. Since $\mathcal{X}_\ell \subseteq \mathcal{X}_\infty$, we infer that $\mathbf{U}_\ell^\star$ is, in fact, also a Galerkin approximation of $\mathbf{u}_\infty^\star$. From the quasi-optimality (2.8) of the Galerkin method, we thus obtain

$$|||\mathbf{u}_\infty^\star - \mathbf{U}_\ell^\star||| \lesssim |||\mathbf{u}_\infty^\star - \mathbb{P}_\ell \mathbf{u}||| \xrightarrow{\ell\to\infty} 0,$$

i.e. $\mathbf{U}_\ell^\star$ tends to the limit $\mathbf{u}_\infty^\star$ as $\ell \to \infty$. □

Proof of a priori convergence of $\mathbf{U}_\ell$. We first show the a priori convergence of the approximate data:

- Applying Lemma 5.3 to $H = L^2(\Gamma_N)$ and $X_\ell = \mathcal{P}^0(\mathcal{E}_\ell|_{\Gamma_N})$, it follows that the limit $\phi_{N,\infty} := \lim_\ell \Pi_\ell \phi_N \in L^2(\Gamma_N)$ exists. With $\Phi_{N,\ell}$ and $\phi_{N,\infty}$ extended by zero, we see that there even holds

$$\phi_{N,\infty} = \lim_{\ell\to\infty} \Phi_{N,\ell} \quad \text{in } L^2(\Gamma). \tag{5.5}$$

- We apply Lemma 5.3 to $H = L^2(\Gamma)$ and $X_\ell = \mathcal{P}^0(\mathcal{E}_\ell)$. It follows that

$$g := \lim_\ell (I_\ell u_D)' = \lim_\ell \Pi_\ell u_D' \quad \text{in } L^2(\Gamma) \tag{5.6}$$

  exists. In particular, $(I_\ell u_D)'$ is a Cauchy sequence in $L^2(\Gamma)$.
- According to the 1D Sobolev inequality and the Rellich compactness theorem, the norm

$$\|v\| := |v(z_0)| + \|v'\|_{L^2(\Gamma)} \qquad \text{for } v \in H^1(\Gamma)$$

  defines an equivalent norm on $H^1(\Gamma)$, where z_0 is an arbitrary but fixed node of $\mathcal{E}_0$. From $I_\ell u_D(z_0) = u_D(z_0)$ and (5.6), we thus infer that $(I_\ell u_D)$ is a Cauchy sequence with respect to $\|\cdot\|$. Consequently, the limit

$$u_{D,\infty} := \lim_{\ell\to\infty} I_\ell u_D \quad \text{in } H^1(\Gamma) \tag{5.7}$$

  exists.

Second, we consider an auxiliary problem with (non-perturbed) data $(u_{D,\infty}, \phi_{N,\infty}) \in H^1(\Gamma) \times L^2(\Gamma)$. Let $\mathbf{U}^\star_{\infty,\ell} \in \mathcal{X}_\ell$ denote the non-perturbed Galerkin solution (2.7) with respect to these data. We have already proven before that the a priori limit

$$\mathbf{u}_\infty = \lim_{\ell\to\infty} \mathbf{U}^\star_{\infty,\ell} \quad \text{in } \mathcal{H} \tag{5.8}$$

exists. We now use the triangle inequality to see

$$|||\mathbf{u}_\infty - \mathbf{U}_\ell||| \le |||\mathbf{u}_\infty - \mathbf{U}^\star_{\infty,\ell}||| + |||\mathbf{U}^\star_{\infty,\ell} - \mathbf{U}_\ell|||. \tag{5.9}$$

By definition of $\mathbf{u}_\infty$, the first term tends to zero as $\ell \to \infty$. The second one can be bounded by stability of Galerkin schemes,

$$|||\mathbf{U}^\star_{\infty,\ell} - \mathbf{U}_\ell||| \lesssim \|u_{D,\infty} - U_{D,\ell}\|_{H^{1/2}(\Gamma)} + \|\phi_{N,\infty} - \Phi_{N,\ell}\|_{H^{-1/2}(\Gamma)}. \tag{5.10}$$

Due to (5.5) and (5.7), the upper bound tends to zero as $\ell \to \infty$. Combining (5.8)–(5.10), we thus conclude $\lim_\ell \mathbf{U}_\ell = \mathbf{u}_\infty$. □

We stress that the preceding proposition does not provide additional information on the a priori limits, and $\mathbf{u}_\infty$ as well as $\mathbf{u}^\star_\infty$ do not coincide in general. Additional information, however, is provided by the following convergence result.

Theorem 5.4. *Algorithm 5.1 guarantees convergence of the error estimator*

$$\lim_{\ell\to\infty} \varrho_\ell = 0. \tag{5.11}$$

Moreover, the following limits exist and coincide

$$\lim_{\ell\to\infty} \mathbf{U}_\ell = \lim_{\ell\to\infty} \mathbf{U}^\star_\ell = \lim_{\ell\to\infty} \widehat{\mathbf{U}}_\ell = \lim_{\ell\to\infty} \widehat{\mathbf{U}}^\star_\ell. \tag{5.12}$$

Under the saturation assumption (2.11) *for the non-perturbed problem, we thus obtain convergence of the perturbed adaptive BEM, i.e.*

$$\lim_{\ell\to\infty} |||\mathbf{u} - \mathbf{U}_\ell||| = 0 = \lim_{\ell\to\infty} |||\mathbf{u} - \widehat{\mathbf{U}}_\ell|||. \tag{5.13}$$

Proof. For arbitrary $\delta > 0$, the Young inequality yields

$$\begin{aligned}
\varrho^2_{\ell+1} \le{}& (1+\delta)\big\{\|h^{1/2}_{\ell+1}(1-\Pi_{\ell+1})\widehat{U}'_{N,\ell}\|^2_{L^2(\Gamma_N)} + \|h^{1/2}_{\ell+1}(1-\Pi_{\ell+1})\widehat{\Phi}_{D,\ell}\|^2_{L^2(\Gamma_D)} \\
&+ \|h^{1/2}_{\ell+1}(1-\Pi_{\ell+1})u'_D\|^2_{L^2(\Gamma_D)} + \|h^{1/2}_{\ell+1}(1-\Pi_{\ell+1})\phi_N\|^2_{L^2(\Gamma_N)}\big\} \\
&+ (1+\delta^{-1})\big\{\|h^{1/2}_{\ell+1}(1-\Pi_{\ell+1})(\widehat{U}_{N,\ell+1} - \widehat{U}_{N,\ell})'\|^2_{L^2(\Gamma_N)} \\
&+ \|h^{1/2}_{\ell+1}(1-\Pi_{\ell+1})(\widehat{\Phi}_{D,\ell+1} - \widehat{\Phi}_{D,\ell})\|^2_{L^2(\Gamma_D)}\big\}.
\end{aligned}$$

Recall that the projection $\Pi_{\ell+1}$ is even the $\mathcal{E}_{\ell+1}$-elementwise L^2-projection. Therefore, the inverse estimates (3.8)–(3.9) and norm equivalence on $\widetilde{H}^{-1/2}(\Gamma_D)$ and $\widetilde{H}^{1/2}(\Gamma_N)$ yield

$$\begin{aligned}
\|h^{1/2}_{\ell+1}(1-\Pi_{\ell+1})(\widehat{U}_{N,\ell+1} - \widehat{U}_{N,\ell})'\|_{L^2(\Gamma_N)} &\le \|h^{1/2}_{\ell+1}(\widehat{U}_{N,\ell+1} - \widehat{U}_{N,\ell})'\|_{L^2(\Gamma_N)} \\
&\le C_{\mathrm{inv}}\|\widehat{U}_{N,\ell+1} - \widehat{U}_{N,\ell}\|_{W(\Gamma_N)}
\end{aligned}$$

and

$$\begin{aligned}
\|h^{1/2}_{\ell+1}(1-\Pi_{\ell+1})(\widehat{\Phi}_{D,\ell+1} - \widehat{\Phi}_{D,\ell})\|_{L^2(\Gamma_D)} &\le \|h^{1/2}_{\ell+1}(\widehat{\Phi}_{D,\ell+1} - \widehat{\Phi}_{D,\ell})\|_{L^2(\Gamma_D)} \\
&\le c_{\mathrm{inv}}\|\widehat{\Phi}_{D,\ell+1} - \widehat{\Phi}_{D,\ell}\|_{V(\Gamma_D)}.
\end{aligned}$$

Clearly, there holds $\|(1-\Pi_{\ell+1})v\|_{L^2(E)} \le \|(1-\Pi_\ell)v\|_{L^2(E)}$, for all $E \in \mathcal{E}_\ell$ and $v \in L^2(E)$. For marked elements $E \in \mathcal{M}_\ell$, we additionally observe $h_{\ell+1}|_E \le (1/2)\, h_\ell|_E$ as well as $\widehat{U}'_\ell|_E, \widehat{\Phi}_\ell|_E \in \mathcal{P}^0(\mathcal{E}_{\ell+1}|_E)$. Therefore, we obtain for $E \in \mathcal{M}_\ell$

$$\begin{aligned}
\Lambda(E) &:= \|h_{\ell+1}^{1/2}(1-\Pi_{\ell+1})\widehat{U}'_{N,\ell}\|^2_{L^2(E\cap\Gamma_N)} + \|h_{\ell+1}^{1/2}(1-\Pi_{\ell+1})\widehat{\Phi}_{D,\ell}\|^2_{L^2(E\cap\Gamma_D)} \\
&\qquad + \|h_{\ell+1}^{1/2}(1-\Pi_{\ell+1})u'_D\|^2_{L^2(E\cap\Gamma_D)} + \|h_{\ell+1}^{1/2}(1-\Pi_{\ell+1})\phi_N\|^2_{L^2(E\cap\Gamma_N)} \\
&\le \frac{1}{2}\big(\|h_\ell^{1/2}(1-\Pi_\ell)u'_D\|^2_{L^2(E\cap\Gamma_D)} + \|h_\ell^{1/2}(1-\Pi_\ell)\phi_N\|^2_{L^2(E\cap\Gamma_N)}\big) \\
&\le \frac{1}{2}\varrho_\ell(E)^2.
\end{aligned}$$

Contrary, for $E \in \mathcal{E}_\ell \setminus \mathcal{M}_\ell$, there holds $h_{\ell+1}|_E \le h_\ell|_E$ and consequently $\Lambda(E) \le \varrho_\ell(E)^2$. Splitting the elements into marked and nonmarked elements, we thus infer

$$\begin{aligned}
&\|h_{\ell+1}^{1/2}(1-\Pi_{\ell+1})\widehat{U}'_{N,\ell}\|^2_{L^2(\Gamma_N)} + \|h_{\ell+1}^{1/2}(1-\Pi_{\ell+1})\widehat{\Phi}_{D,\ell}\|^2_{L^2(\Gamma_D)} \\
&\qquad + \|h_{\ell+1}^{1/2}(1-\Pi_{\ell+1})u'_D\|^2_{L^2(\Gamma_D)} + \|h_{\ell+1}^{1/2}(1-\Pi_{\ell+1})\phi_N\|^2_{L^2(\Gamma_N)} \\
&\le \frac{1}{2}\sum_{E\in\mathcal{M}_\ell}\varrho_\ell(E)^2 + \sum_{E\in\mathcal{E}_\ell\setminus\mathcal{M}_\ell}\varrho_\ell(E)^2 \\
&= \varrho_\ell^2 - \frac{1}{2}\sum_{E\in\mathcal{M}_\ell}\varrho_\ell(E)^2 \\
&\le (1-\theta/2)\varrho_\ell^2,
\end{aligned}$$

where we have finally used the Dörfler marking (5.3). Altogether, we thus have shown

$$\varrho_{\ell+1}^2 \le (1+\delta)(1-\theta/2)\varrho_\ell^2 + (1+\delta^{-1})\max\{c_{\mathrm{inv}}^2, C_{\mathrm{inv}}^2\}\,|||\widehat{\mathbf{U}}_{\ell+1} - \widehat{\mathbf{U}}_\ell|||^2 \tag{5.14}$$

By choosing $\delta > 0$ sufficiently small, we guarantee that $q := (1+\delta)(1-\theta/2) < 1$. Recall that Proposition 5.2 predicts that all limits in (5.12) exist. In particular, $\lim_\ell |||\widehat{\mathbf{U}}_{\ell+1} - \widehat{\mathbf{U}}_\ell||| = 0$. An estimate of the type (5.14) is called *estimator reduction* in [3], and elementary calculus yields $\lim_\ell \varrho_\ell = 0$, see [3, Lemma 2.3]. This concludes the proof of (5.11).

Recall that $\varrho_\ell^2 = \mu_\ell^2 + \mathrm{osc}_\ell^2 \to 0$ as $\ell \to \infty$. With $\lim_\ell \mathrm{osc}_\ell = 0$, there holds $u_{D,\infty} := \lim_\ell U_{D,\ell} = u_D \in H^1(\Gamma)$ as well as $\phi_{N,\infty} := \lim_\ell \Phi_{N,\ell} = \phi_N \in L^2(\Gamma)$. In particular, the proof of Proposition 5.2 reveals $\mathbf{u}_\infty = \mathbf{u}_\infty^\star$ as well as $\widehat{\mathbf{u}}_\infty = \widehat{\mathbf{u}}_\infty^\star$ for the a priori limits of $\mathbf{U}_\ell$, $\mathbf{U}_\ell^\star$, $\widehat{\mathbf{U}}_\ell$, and $\widehat{\mathbf{U}}_\ell^\star$, respectively. Moreover, the estimate

$$\eta_\ell^\star = |||\widehat{\mathbf{U}}_\ell^\star - \mathbf{U}_\ell^\star||| \lesssim \mu_\ell^\star \lesssim \varrho_\ell \xrightarrow{\ell\to\infty} 0$$

proves $\widehat{\mathbf{u}}_\infty = \mathbf{u}_\infty$, see proof of Theorem 4.1. This concludes the proof of (5.12). □

6. Non-homogeneous volume forces

6.1. Continuous model with volume forces. In the preceding sections, we restricted ourselves to nonhomogenous volume forces for the ease of presentation. In the following, we comment on the extension of the PDE model problem which now reads

$$\left\{\begin{array}{rcll} -\Delta u &=& f & \text{in } \Omega, \\ u &=& u_D & \text{on } \Gamma_D, \\ \partial_n u &=& \phi_N & \text{on } \Gamma_N. \end{array}\right. \tag{6.1}$$

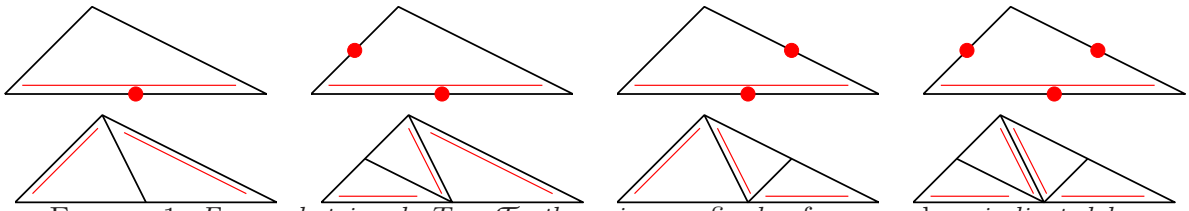

FIGURE 1. *For each triangle $T \in \mathcal{T}$, there is one fixed* reference edge, *indicated by the double line (left, top). Refinement of T is done by bisecting the reference edge, where its midpoint becomes a new node. The reference edges of the son triangles are opposite to this newest vertex (left, bottom). To avoid hanging nodes, one proceeds as follows: We assume that certain edges of T, but at least the reference edge, are marked for refinement (top). Using iterated newest vertex bisection, the element is then split into 2, 3, or 4 son triangles (bottom).*

Besides the aforegoing assumptions, the new formulation involves some volume force $f \in \widetilde{H}^{-1}(\Omega)$. In the integral formulation (2.2), this only leads to an extended right-hand side

$$F := (1/2 - A) \begin{pmatrix} u_D \\ \phi_N \end{pmatrix} - \begin{pmatrix} N_0 f \\ N_1 f \end{pmatrix}, \tag{6.2}$$

where $N_0 f$ and $N_1 f$ denote the trace and the normal derivative of the Newton potential, which is formally defined by

$$Nf(x) := -\frac{1}{2\pi} \int_\Omega \log|x-y| f(y)\, dy \quad \text{for } x \in \Omega. \tag{6.3}$$

We recall the mapping properties $N_0 \in L(\widetilde{H}^{-1}(\Omega), H^{1/2}(\Gamma))$ and $N_1 \in L(\widetilde{H}^{-1/2}(\Omega), H^{-1/2}(\Gamma))$ from [25, 29, 30]. Moreover, it is well-known that there holds the identity

$$N_1 = (-1/2 + K')V^{-1} N_0 \tag{6.4}$$

which is a consequence of the Calderón projector, see e.g. [30, Lemma 6.20].

6.2. Discretization of volume contributions. We assume that the volume forces satisfy the additional regularity assumption $f \in L^2(\Omega)$. Let $\mathcal{T}_\ell$ be a partition of Ω into regular convex cells. The same arguments as in [8, Theorem 4.1] then prove

$$\|f - \pi_\ell f\|_{\widetilde{H}^{-1}(\Omega)} \le \widetilde{C}_{\mathrm{apx}} \, \|h_\ell (1 - \pi_\ell) f\|_{L^2(\Omega)}, \tag{6.5}$$

where π_ℓ denotes the L^2-orthogonal projection onto the $\mathcal{T}_\ell$-piecewise constants $\mathcal{P}^0(\mathcal{T}_\ell)$ and where h_ℓ is the local mesh-width defined by $h_\ell|_T = \mathrm{area}(T)^{1/2}$ for all $T \in \mathcal{T}_\ell$. The constant $\widetilde{C}_{\mathrm{apx}} > 0$ only depends on the shape regularity of $\mathcal{T}_\ell$.

Although not necessary in theory, we assume that $\mathcal{T}_\ell$ is a regular triangulation of Ω into non-degenerate triangles, and refinement of an element $T \in \mathcal{T}_\ell$ will be done by newest vertex bisection, cf. Figure 1. The reader is also referred to [33, Chapter 4] for further details on local mesh-refinement. For implementational simplicity, we will ensure that the boundary mesh $\mathcal{E}_\ell$ is the restriction of the volume mesh, i.e. $\mathcal{E}_\ell = \mathcal{T}_\ell|_\Gamma$. We note that newest vertex bisection leads to uniformly shape regular meshes. By definition of $\mathcal{E}_\ell$, this implies uniform boundedness of the local mesh-ratio $\sup_{\ell \in \mathbb{N}} \kappa(\mathcal{E}_\ell) < \infty$.

For the computation of the perturbed Galerkin solution, we replace $N_0 f$ by $N_0(\pi_\ell f)$, and an approximation of $N_1 f$ is obtained with the help of (6.4) as follows: We consider the first-kind integral equation

$$\langle V\nu, \chi\rangle = \langle N_0 f, \chi\rangle \quad \text{for all } \chi \in H^{-1/2}(\Gamma) \tag{6.6}$$

and recall that V is a symmetric and elliptic operator between $H^{-1/2}(\Gamma)$ and $H^{1/2}(\Gamma)$. Therefore, there is a unique solution $\nu = V^{-1}N_0 f \in H^{-1/2}(\Gamma)$ and (6.4) yields $N_1 f = (-1/2 + K')\nu$.

Our discrete scheme now reads as follows: In a first step, we compute the unique Galerkin solution $N_\ell \in \mathcal{P}^0(\mathcal{E}_\ell)$ of (6.6) with respect to the perturbed right-hand side given by $\pi_\ell f$, i.e.

$$\langle V N_\ell \,, X_\ell \rangle = \langle N_0(\pi_\ell f) \,, X_\ell \rangle \quad \text{for all } X_\ell \in \mathcal{P}^0(\mathcal{E}_\ell). \tag{6.7}$$

With this N_ℓ, the new approximate right-hand side takes the form

$$F_\ell := (1/2 - A) \begin{pmatrix} I_\ell u_D \\ \Pi_\ell \phi_N \end{pmatrix} - \begin{pmatrix} N_0(\pi_\ell f) \\ (-1/2 + K')N_\ell \end{pmatrix}. \tag{6.8}$$

In a second step, we then compute the perturbed Galerkin solution $\mathbf{U}_\ell = (U_{N,\ell}, \Phi_{D,\ell}) \in \mathcal{X}_\ell$ by solving (2.10).

6.3. Extended error estimator. In addition to (2.11), we assume the saturation assumption

$$\|\nu - \widehat{N}_\ell^\star\|_{V(\Gamma)} \le C_{\rm sat} \, \|\nu - N_\ell^\star\|_{V(\Gamma)}, \tag{6.9}$$

where $N_\ell^\star \in \mathcal{P}^0(\mathcal{E}_\ell)$ and $\widehat{N}_\ell^\star \in \mathcal{P}^0(\widehat{\mathcal{E}}_\ell)$ are the Galerkin solutions of (6.6) with respect to the non-perturbed right-hand side $N_0 f$.

Now, the error estimator μ_ℓ takes the form

$$\mu_\ell^2 := \|h_\ell^{1/2}(1 - \Pi_\ell)\widehat{U}'_{N,\ell}\|^2_{L^2(\Gamma_N)} + \|h_\ell^{1/2}(1 - \Pi_\ell)\widehat{\Phi}_{D,\ell}\|^2_{L^2(\Gamma_D)} + \|h_\ell^{1/2}(1 - \Pi_\ell)\widehat{N}_\ell\|^2_{L^2(\Gamma)}, \tag{6.10}$$

and the data oscillations read

$$\operatorname{osc}_\ell^2 := \|h_\ell^{1/2}(1 - \Pi_\ell)u'_D\|^2_{L^2(\Gamma_D)} + \|h_\ell^{1/2}(1 - \Pi_\ell)\phi_N\|^2_{L^2(\Gamma_N)} + \|h_\ell \, (1 - \pi_\ell)f\|^2_{L^2(\Omega)}. \tag{6.11}$$

With this notation, the following analogon of Theorem 4.2 still holds.

Theorem 6.1. *There is a constant $C_6 > 0$ which only depends on Γ_D, Γ_N, $\kappa(\mathcal{E}_\ell)$, and the saturation assumptions* (2.11) *as well as* (6.9) *such that*

$$C_6^{-1} \, |||\mathbf{u} - \mathbf{U}_\ell||| \le \varrho_\ell := (\mu_\ell^2 + \operatorname{osc}_\ell^2)^{1/2}, \tag{6.12}$$

i.e. ϱ_ℓ is a reliable error estimator.

Sketch of Proof. Recall that $\|\cdot\|_{H^{-1/2}(\Gamma_N)} \le \|\cdot\|_{H^{-1/2}(\Gamma)}$. Using this and $N_1 f = (-1/2 + K')\nu$, we can apply the triangle inequality and the continuity of the operator $(-1/2 + K')$ to obtain

$$\begin{aligned} \|N_1 f - (-1/2 + K')N_\ell\|_{H^{-1/2}(\Gamma_N)} &\le \|N_1 f - (-1/2 + K')N_\ell\|_{H^{-1/2}(\Gamma)} \\ &\le \|(-1/2 + K')(\nu - N_\ell^\star)\|_{H^{-1/2}(\Gamma)} + \|(-1/2 + K')(N_\ell^\star - N_\ell)\|_{H^{-1/2}(\Gamma)} \\ &\lesssim \|\nu - N_\ell^\star\|_{V(\Gamma)} + \|N_\ell^\star - N_\ell\|_{V(\Gamma)}. \end{aligned}$$

With the saturation assumption (6.9) and the same arguments as in the proof of Theorem 4.2, there holds

$$\|\nu - N_\ell^\star\|_{V(\Gamma)} \lesssim \|h_\ell^{1/2}(\widehat{N}_\ell - N_\ell)\|_{L^2(\Gamma)} + \operatorname{osc}_\ell \quad \text{as well as} \quad \|N_\ell^\star - N_\ell\|_{V(\Gamma)} \lesssim \operatorname{osc}_\ell.$$

Therefore, the consistency error in the right-hand side F_ℓ, measured in the dual space $\mathcal{H}^*$, is bounded by

$$|||F - F_\ell|||_{\mathcal{H}^*} \lesssim \|h_\ell^{1/2}(\widehat{N}_\ell - N_\ell)\|_{L^2(\Gamma)} + \operatorname{osc}_\ell.$$

From this, we derive reliability (6.12). □

Remark 3. *If we change the notion of the error and consider the triple* $\mathbf{u} := (u_N, \phi_D, \nu) \in \mathcal{H} := \widetilde{H}^{1/2}(\Gamma_N) \times \widetilde{H}^{-1/2}(\Gamma_D) \times H^{-1/2}(\Gamma)$ *and its approximate solution* $\mathbf{U}_\ell := (U_{N,\ell}, \Phi_{D,\ell}, N_\ell) \in \mathcal{X}_\ell := \mathcal{S}^1_0(\mathcal{E}_\ell|_{\Gamma_N}) \times \mathcal{P}^0(\mathcal{E}_\ell|_{\Gamma_D}) \times \mathcal{P}^0(\mathcal{E}_\ell)$*, we can in fact prove that the error estimator* $\varrho_\ell^2 = \mu_\ell^2 + \operatorname{osc}_\ell^2$ *is efficient and reliable up to data oscillations. The details are analogous to Theorem 4.2.* □

6.4. A convergent adaptive algorithm. The adaptive mesh-refinement is now steered by the refinement indicators

$$\varrho_\ell(\tau)^2 := \begin{cases} \|h_\ell^{1/2}(\widehat{U}_{N,\ell} - I_\ell \widehat{U}_{N,\ell})'\|^2_{L^2(E)} + \|h_\ell^{1/2}(\phi_N - \Pi_\ell \phi_N)\|^2_{L^2(E)} \\ \qquad + \|h_\ell^{1/2}(\widehat{N}_\ell - \Pi_\ell \widehat{N}_\ell)\|^2_{L^2(E)} & \text{for } \tau = E \in \mathcal{E}_\ell \text{ with } E \subseteq \Gamma_N, \\ \|h_\ell^{1/2}(\widehat{\Phi}_{D,\ell} - \Pi_\ell \widehat{\Phi}_{D,\ell})\|^2_{L^2(E)} + \|h_\ell^{1/2}(u_D - I_\ell u_D)'\|^2_{L^2(E)} \\ \qquad + \|h_\ell^{1/2}(\widehat{N}_\ell - \Pi_\ell \widehat{N}_\ell)\|_{L^2(E)} & \text{for } \tau = E \in \mathcal{E}_\ell \text{ with } E \subseteq \Gamma_D, \\ \|h_\ell\,(f - \pi_\ell f)\|^2_{L^2(T)} & \text{for } \tau = T \in \mathcal{T}_\ell, \end{cases}$$

defined for all $\tau \in \mathcal{E}_\ell \cup \mathcal{T}_\ell$. Note that

$$\sum_{\tau \in \mathcal{E}_\ell \cup \mathcal{T}_\ell} \varrho_\ell(\tau)^2 = \mu_\ell^2 + \operatorname{osc}_\ell^2 = \varrho_\ell^2. \tag{6.13}$$

As above, these indicators are used to mark certain elements $\mathcal{M}_\ell \subseteq \mathcal{E}_\ell \cup \mathcal{T}_\ell$ by use of the Dörfler marking (6.14). The adaptive algorithm takes the following form:

Algorithm 6.2. INPUT*: Initial triangulation* $\mathcal{T}_0$ *of* Ω *and initial boundary partition* $\mathcal{E}_0 := \mathcal{T}_0|_\Gamma$*, adaptivity parameter* $\theta \in (0, 1]$*, and counter* $\ell := 0$*.*

(i) *Construct uniform refinement* $\widehat{\mathcal{T}}_\ell$ *of* $\mathcal{T}_\ell$ *and define boundary mesh* $\widehat{\mathcal{E}}_\ell := \widehat{\mathcal{T}}_\ell|_\Gamma$*.*
(ii) *Compute Galerkin solution* $\widehat{N}_\ell \in \mathcal{P}^0(\widehat{\mathcal{E}}_\ell)$ *and perturbed right-hand side* F_ℓ*.*
(iii) *Compute Galerkin solution* $\widehat{\mathbf{U}}_\ell = (\widehat{U}_{N,\ell}, \widehat{\Phi}_{D,\ell}) \in \widehat{\mathcal{X}}_\ell := \mathcal{S}^1_0(\widehat{\mathcal{E}}_\ell|_{\Gamma_N}) \times \mathcal{P}^0(\widehat{\mathcal{E}}_\ell|_{\Gamma_D})$*.*
(iv) *Compute refinement indicators* $\varrho_\ell(\tau)$ *for all* $\tau \in \mathcal{E}_\ell \cup \mathcal{T}_\ell$*.*
(v) *Determine minimal set* $\mathcal{M}_\ell \subseteq \mathcal{E}_\ell \cup \mathcal{T}_\ell$ *such that*

$$\theta\, \varrho_\ell^2 \le \sum_{\tau \in \mathcal{M}_\ell} \varrho_\ell(\tau)^2. \tag{6.14}$$

(vi) *Mark edges* $E \in \mathcal{E}_\ell \cap \mathcal{M}_\ell$ *for refinement. For marked elements* $T \in \mathcal{T}_\ell \cap \mathcal{M}_\ell$*, mark their reference edge for refinement.*
(vii) *Use newest vertex bisection to generate a new mesh* $\mathcal{T}_{\ell+1}$*.*
(viii) *Increase counter* $\ell \mapsto \ell + 1$ *and go to* (i)*.*

OUTPUT*: Sequences of volume meshes* $\mathcal{T}_\ell$*, discrete solutions* $\widehat{\mathbf{U}}_\ell$ *as well as* $\widehat{N}_\ell$ *on* $\mathcal{E}_\ell := \mathcal{T}_\ell|_\Gamma$*, and corresponding estimators* $\varrho_\ell = (\mu_\ell^2 + \operatorname{osc}_\ell^2)^{1/2}$*.* □

Remark 4. *First, recall that newest vertex bisection of a volume mesh guarantees*

$$\#\mathcal{T}_\ell - \#\mathcal{T}_0 \le C_{\mathrm{mark}} \sum_{j=0}^{\ell-1} \#\mathcal{M}_j, \tag{6.15}$$

where $\mathcal{M}_j$ *may be an arbitrary subset of* $\mathcal{T}_j$*, cf.* [6, 32]*. The constant* $C_{\mathrm{mark}} > 0$ *only depends on the initial mesh* $\mathcal{T}_0$ *and the assumption that each interior edge* $E = E_+ \cap E_-$ *with* $E_+, E_- \in E$ *is the refinement edge of* E_+ *if and only if it is also the refinement*

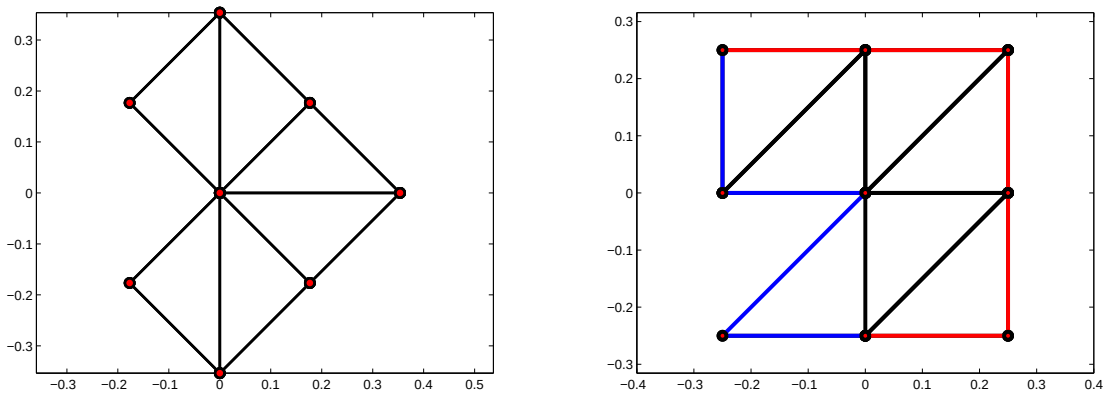

FIGURE 2. *Boundary Γ and initial meshes $\mathcal{E}_0$ and $\mathcal{T}_0$ in Examples 7.1 and 7.2 (left) as well as boundary Γ and initial meshes $\mathcal{E}_0$ and $\mathcal{T}_0$ in Example 7.3 (right). Here, the blue part is the Dirichlet boundary Γ_D and the red part is the Neumann boundary Γ_N.*

edge of E_-. See [6] *for a proof that an initial marking of this kind can always be guaranteed. Second, recall that marked volume elements are bisected along the refinement edge. Therefore, additional marking of boundary edges only results in marking several edges of an element. Therefore,* (6.15) *also holds for our adaptive strategy if $\mathcal{M}_j \subseteq \mathcal{E}_j \cup \mathcal{T}_j$ is interpreted as set of marked edges.* □

Analogously to Theorem 5.4, we have the following convergence result. The proof follows the ideas given above and is thus omitted.

Theorem 6.3. *Algorithm 6.2 guarantees convergence of the error estimator*

$$\lim_{\ell\to\infty} \varrho_\ell = 0. \tag{6.16}$$

Moreover, the following limits exist and coincide

$$\lim_{\ell\to\infty} \mathbf{U}_\ell = \lim_{\ell\to\infty} \mathbf{U}_\ell^\star = \lim_{\ell\to\infty} \widehat{\mathbf{U}}_\ell = \lim_{\ell\to\infty} \widehat{\mathbf{U}}_\ell^\star. \tag{6.17}$$

Under the saturation assumptions (2.11) *and* (6.9)*, this leads to*

$$\lim_{\ell\to\infty} |||\mathbf{u} - \mathbf{U}_\ell||| = 0 = \lim_{\ell\to\infty} |||\mathbf{u} - \widehat{\mathbf{U}}_\ell|||, \tag{6.18}$$

i.e. convergence of the adaptive scheme. Moreover, there holds $\lim_{\ell\to\infty} \|\nu - N_\ell\|_{H^{-1/2}(\Gamma)} = 0$. □

7. Numerical experiments

In this section, we comment on three numerical experiments with non-homogenous volume force $f \neq 0$. Our implementation uses the MATLAB BEM library `HILBERT` [2] which includes black-box implementations of the assembly of the Galerkin data as well as of error estimators and data oscillations.

Throughout, the volume mesh $\mathcal{T}_\ell$ and the boundary mesh $\mathcal{E}_\ell$ are coupled in the sense that $\mathcal{E}_\ell$ is the restriction of $\mathcal{T}_\ell$ to the boundary. Although not mandatory for our analysis, this restriction eases the stable computation of $N_0\pi_\ell f$. We recall that Algorithm 6.2 uses an edge-based refinement strategy based on newest vertex bisection, which ensures $\mathcal{T}_\ell|_\Gamma = \mathcal{E}_\ell$.

In order to emphasize the performance of our adaptive algorithm we compare its behaviour and efficiency with that of a uniform approach. Uniform refinements are obtained

by marking all edges of the volume-mesh $\mathcal{T}_\ell$, i.e.: all triangles are bisected by three bisections (see Figure 1 right) and, in particular, all boundary elements are halved.

The results of each experiment are visualized with three pictures to compare the performance of the uniform and adaptive algorithm with respect to the empirical order of convergence and the use of system resources. Each picture may include plots of the following quantities:

- the error estimate $\mu_\ell^2(\Gamma) := \|h_\ell^{1/2}(1-\Pi_\ell)\widehat{U}'_{N,\ell}\|^2_{L^2(\Gamma_N)} + \|h_\ell^{1/2}(1-\Pi_\ell)\widehat{\Phi}_{D,\ell}\|^2_{L^2(\Gamma_D)}$,
- the error estimate $\mu_\ell^2(\Omega) := \|h_\ell^{1/2}(1-\Pi_\ell)\widehat{N}_\ell\|^2_{L^2(\Gamma)}$
- the boundary data oscillations $\operatorname{osc}_\ell^2(\Gamma) := \|h_\ell^{1/2}(1-\Pi_\ell)u'_D\|^2_{L^2(\Gamma_D)} + \|h_\ell^{1/2}(1-\Pi_\ell)\phi_N\|^2_{L^2(\Gamma_N)}$
- the volume data oscillations $\operatorname{osc}_\ell^2(\Omega) := \|h_\ell\,(1-\pi_\ell)f\|^2_{L^2(\Omega)}$.

We stress that $\mu_\ell(\Omega)$ has only to be taken into account, if the normal derivative $N_1 f$ has to be computed, see Section 6. Furthermore, since we prescribe the exact solutions in our experiments, we can compute a reliable error bound err_ℓ as follows: First, triangle inequality and best approximation property of Galerkin solutions yield

$$|||\mathbf{u}-\mathbf{U}_\ell||| \le |||\mathbf{u}-\mathbf{U}_\ell^\star||| + |||\mathbf{U}_\ell-\mathbf{U}_\ell^\star||| \le |||\mathbf{u}-(I_\ell u_N, \Pi_\ell\phi_D)||| + |||\mathbf{U}_\ell-\mathbf{U}_\ell^\star|||$$

Second, we use $|||\mathbf{U}_\ell-\mathbf{U}_\ell^\star||| \lesssim \operatorname{osc}_\ell(\Gamma)+\operatorname{osc}_\ell(\Omega)$. Third, from (3.6), (3.10), and (3.13) and the fact that I_ℓ as well as Π_ℓ are projections, we conclude

$$\begin{aligned}|||\mathbf{u}-(I_\ell u_N,\Pi_\ell\phi_D)||| &\lesssim \|u_N - I_\ell u_N\|_{W(\Gamma_N)} + \|\phi_D-\Pi_\ell\phi_D\|_{V(\Gamma_D)}\\ &\lesssim \|h_\ell^{1/2}(u_N-U_{N,\ell})'\|_{L^2(\Gamma_N)} + \|h_\ell^{1/2}(\phi_D-\Phi_{D,\ell})\|_{L^2(\Gamma_D)}.\end{aligned}$$

Therefore, a reliable error bound is given by

$$\begin{aligned}|||\mathbf{u}-\mathbf{U}_\ell||| &\lesssim \operatorname{osc}_\ell(\Gamma)+\operatorname{osc}_\ell(\Omega) + \|h_\ell^{1/2}(u_N-U_{N,\ell})'\|_{L^2(\Gamma_N)} + \|h_\ell^{1/2}(\phi_D-\Phi_{D,\ell})\|_{L^2(\Gamma_D)}\\ &=: \operatorname{err}_\ell.\end{aligned}$$

The error bound err_ℓ is plotted throughout for reference.

In order to study the convergence behaviour of our adaptive approach, we plot all quantities over the number of boundary elements $\#\mathcal{E}_\ell$. We recall that the optimal rate of convergence of lowest-order BEM is $\mathcal{O}(\#\mathcal{E}_\ell^{-3/2})$. The examples are chosen in such a way that uniform mesh-refinement can be predicted to yield a reduced order of convergence.

Furthermore, two critical system resources may be identified: First computational time may be relevant, second consumed memory physically limits the reachable accuracy of a Galerkin discretization. Therefore, we plot the quantities over the computational time. The time consumption is measured differently for uniform and adaptive approach: An adaptively generated solution $\mathbf{U}_\ell$ depends on the entire history of solutions $\mathbf{U}_0,\dots,\mathbf{U}_{\ell-1}$, whereas this is not the case for an uniform approach. To be precise, we define the computational time as follows:

- For uniform mesh-refinement, $t_\ell^{(unif)}$ is the time elapsed for ℓ uniform mesh-refinements of the initial mesh $\mathcal{T}_0$, the assembly of the Galerkin data, and the computation of the Galerkin solution with respect to $\mathcal{E}_\ell$.

For adaptive mesh-refinement, the computational time is defined in an inductive manner:

- We define $t_{-1}^{(adap)} := 0$.
- For $\ell \ge 0$, $t_\ell^{(adap)}$ is the sum of the previous steps $t_{\ell-1}^{(adap)}$ plus the time elapsed for the uniform refinement of $\mathcal{E}_\ell$ to obtain $\widehat{\mathcal{E}}_\ell$, the assembly of the Galerkin data, the computation of the Galerkin solution and the local contributions of the error

indicators, the marking step, and the local refinement of $\mathcal{E}_\ell$ and $\mathcal{T}_\ell$ to obtain $\mathcal{E}_{\ell+1}$ and $\mathcal{T}_{\ell+1}$.

Second, we plot the quantities over the memory consumption which is understood as follows:

- For uniform mesh-refinement, we count the memory which is occupied by the data structure for the boundary- and volume meshes, the discrete integral operators and the solution vector.
- For the adaptive version, we count the memory which is occupied by the data structure for the coarse mesh, the fine mesh, the refined mesh, the integral operators, the error estimators, and the data oscillations which are needed for the adaptive mesh-refinement.

7.1. Dirichlet problem with constant volume force. In our first experiment, we consider the Dirichlet problem $\Gamma_D = \Gamma$ on an L-shaped domain (Figure 2, left) with constant volume force $f \equiv 1$. The domain has a reentrant corner at the origin and is symmetric with respect to the x-axis. The prescribed exact solution of the PDE is given by

$$(x, y) = -\frac{1}{4}(x^2 + y^2) + r^{2/3} \cos(2\varphi/3),$$

were (r, φ) are polar coordinates with respect to the origin. By choice of u, the normal derivative $\phi = \partial_n u$ has a singularity at the reentrant corner. On the other hand, the Dirichlet data $u_D = u|_\Gamma$ are smooth, and one observes optimal decay of the data oscillations $\operatorname{osc}_\ell(\Gamma) = \mathcal{O}(\#\mathcal{E}_\ell^{-3/2})$ even for uniform mesh-refinement. The volume force $f \equiv 1$ is resolved exactly, i.e. $\operatorname{osc}_\ell(\Omega) = 0$, so that we expect no refinement of the volume mesh due to volume data oscillations in the adaptive scheme. Nevertheless, refinement due to coupling of boundary and volume mesh will occur.

In Figure 3, we plot the reliable error bound err_ℓ, the estimator $\mu_\ell(\Gamma)$, and the data oscillations $\operatorname{osc}_\ell(\Gamma)$ for uniform and adaptive approach. As can be predicted theoretically, uniform mesh-refinement leads to a reduced order of convergence of $\mathcal{O}(\#\mathcal{E}_\ell^{-2/3})$ for err_ℓ and μ_ℓ due to the singularity of ϕ. However, the optimal order of convergence is recovered by the adaptive strategy. Moreover, we observe that the adaptive scheme is —at least asymptotically— much superior to the uniform approach with respect to system resources.

7.2. Dirichlet problem with smooth volume force. In our second experiment, we consider the Dirichlet problem $\Gamma_D = \Gamma$ on an L-shaped domain (Figure 2, left) with polynomial volume force $f \in \mathcal{P}^2(\Omega)$. The prescribed exact solution of the PDE is given by

$$u(x, y) = xy(x - \frac{1}{4})(y - \frac{1}{4}) + r^{2/3} \cos(2\varphi/3),$$

with (r, φ) again being polar coordinates with respect to the origin. In contrast to the first experiment, we now expect a certain refinement of the volume mesh due to volume data oscillations in the adaptive scheme. Besides that, we expect the same convergence behaviour of the BEM solution as in Example 7.1 due to the singularity of $\phi = \partial_n u$.

In Figure 4, we plot error bound err_ℓ, the error estimator $\mu_\ell(\Gamma)$ and the data oscillations $\operatorname{osc}_\ell(\Gamma)$ as well as $\operatorname{osc}_\ell(\Omega)$ for uniform and adaptive approach. As can be predicted theoretically, uniform mesh-refinement leads to a reduced order of convergence of $\mathcal{O}(\#\mathcal{E}_\ell^{-2/3})$ for err_ℓ and μ_ℓ due to the singularity of ϕ. However, the optimal order of convergence is recovered by the adaptive strategy. Moreover, we observe that the adaptive scheme is again superior to the uniform approach with respect to system resources.

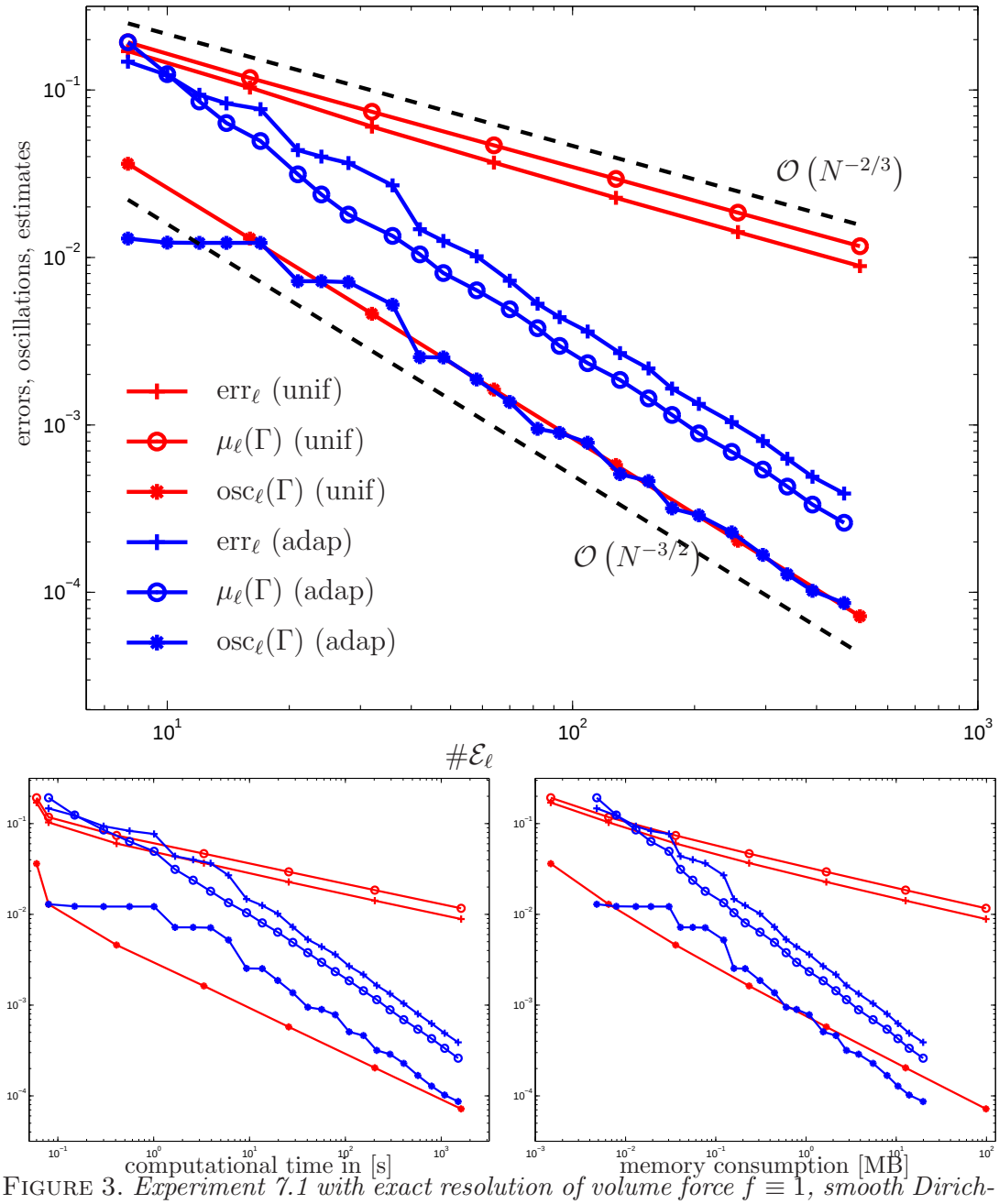

FIGURE 3. *Experiment 7.1 with exact resolution of volume force $f \equiv 1$, smooth Dirichlet data, and singular Neumann data. For uniform mesh-refinement, the singularity of ϕ leads to a reduced order of convergence $\mathcal{O}(\#\mathcal{E}_\ell^{-2/3})$, whereas the adaptive strategy recovers the optimal order of convergence $\mathcal{O}(\#\mathcal{E}_\ell^{-3/2})$. Moreover, the adaptive scheme is also much superior with respect to computational time and memory consumption.*

7.3. Mixed boundary value problem with singular volume force. In our final experiment, we consider a mixed boundary value problem on a Z-shaped domain (Figure 2, right). The Dirichlet boundary Γ_D is indicated in blue, whereas the Neumann boundary Γ_N is indicated in red. The prescribed exact solution of the PDE is given by

$$u(\mathbf{x}) = |\mathbf{x} - \mathbf{z}|^{0.51},$$

where $\mathbf{z} \in \Omega$. By choice of u, the volume force satisfies $f \in H^1(\Omega)\backslash H^2(\Omega)$. Therefore, adaptive mesh-refinement of the volume triangulation is necessary to obtain optimal convergence results. Besides that, the Dirichlet data $u_D = u|_{\Gamma_D}$ as well as the Neumann

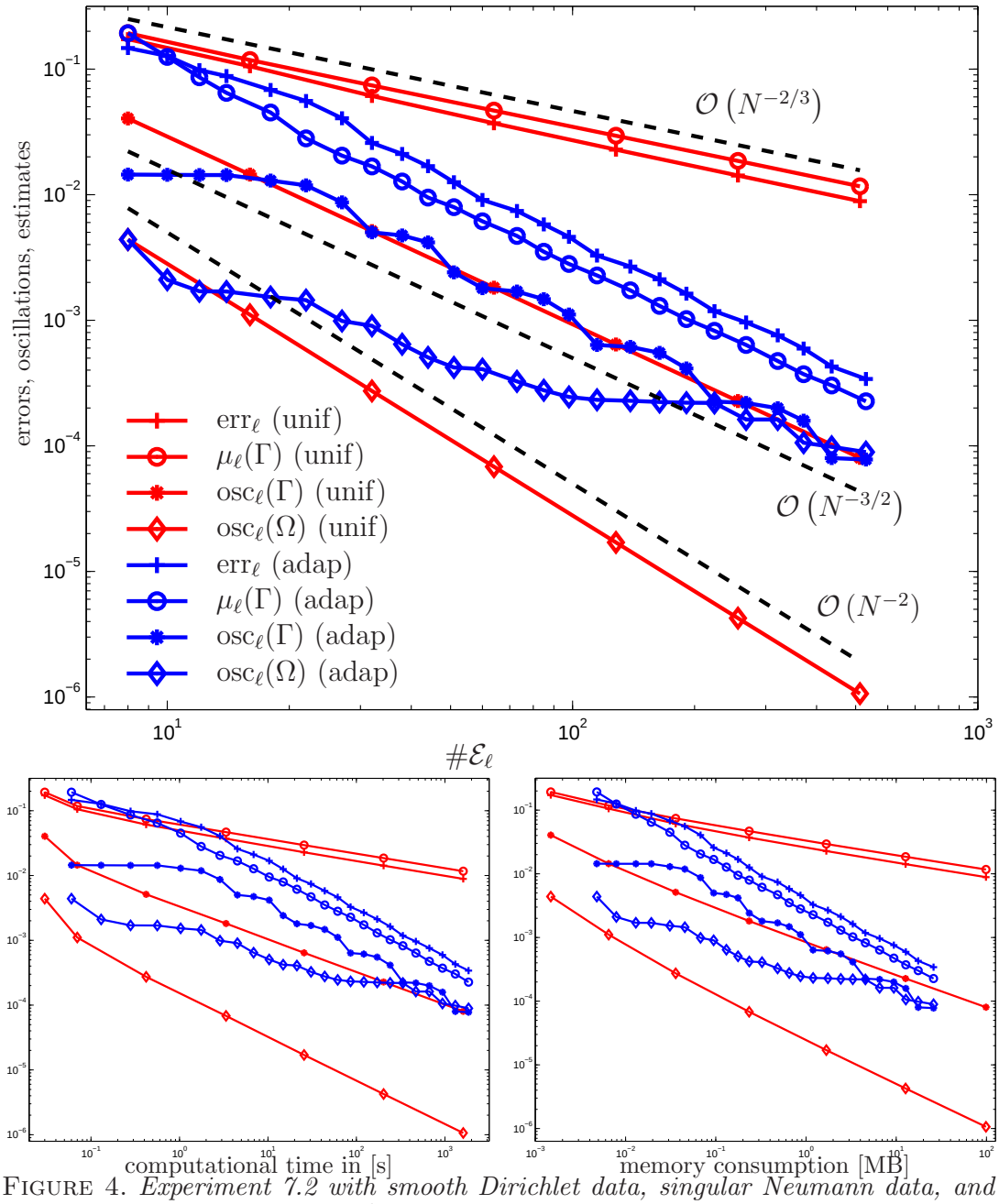

FIGURE 4. *Experiment 7.2 with smooth Dirichlet data, singular Neumann data, and polynomial volume force $f \in \mathcal{P}^2(\Omega)$. As in the first experiment, we expect a reduced order of convergence for uniform mesh-refinement.*

data $\phi_N = \partial_n u|_{\Gamma_N}$ are smooth, and one observes optimal decay of the data oscillations $\mathrm{osc}_\ell(\Gamma) = \mathcal{O}(\#\mathcal{E}_\ell^{-3/2})$ even for uniform mesh-refinement.

In Figure 5, we plot the error bound err_ℓ, the error estimates $\mu_\ell(\Gamma)$ and $\mu_\ell(\Omega)$, the boundary data oscillations $\mathrm{osc}_\ell(\Gamma)$, and the volume data oscillations $\mathrm{osc}_\ell(\Omega)$ for uniform and adaptive approach.

Although ϕ is non-smooth, we observe a reduced order of convergence $\mathcal{O}(\#\mathcal{E}_\ell^{-4/7})$ for uniform mesh-refinement. This is due to the fact the we additionally solve the weakly-singular integral equation (6.6) to approximate $N_1 f$. Here, a generic edge singularity at the reentrant corner seems to occur which dominates the overall convergence behaviour.

Anyway, the optimal order of convergence with respect to $\#\mathcal{E}_\ell$ is recovered by the adaptive algorithm. Besides that, we see that the singularity of the volume force f limits

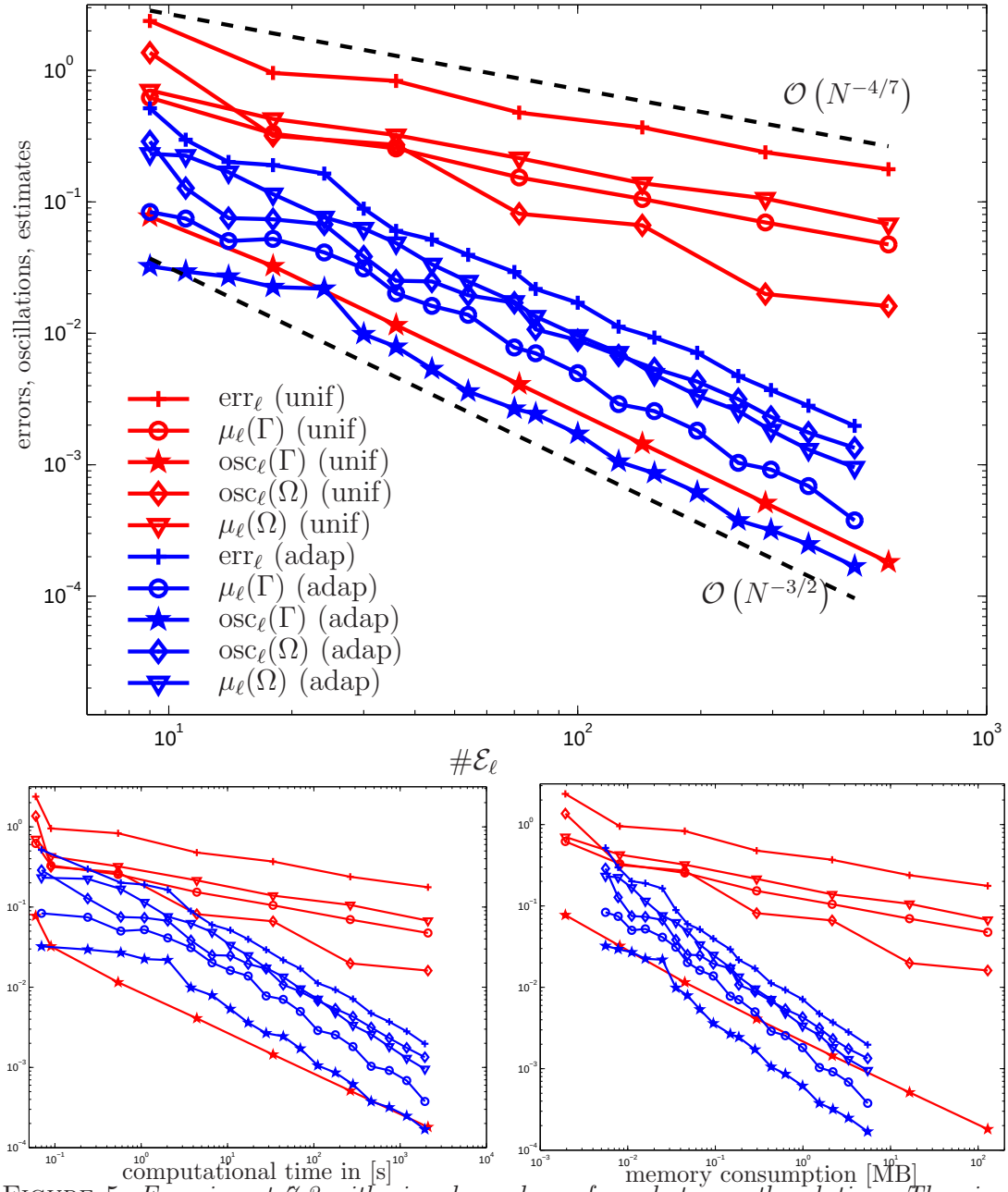

FIGURE 5. *Experiment 7.3 with singular volume force but smooth solution. The singularity of f yields suboptimal usage of memory resources if the volume mesh would not be refined adaptively.*

the efficient use of system resources, even if the boundary mesh would be refined in an optimal manner. On the other hand, since the adaptive scheme even takes care of the volume data oscillations and refines the volume mesh adaptively, we observe that it is superior to the uniform approach with respect to system resources.

Acknowledgement. The second author (SFL) acknowledges a grant of the graduate school *Differential Equations — Models in Science and Engineering*, funded by the Austrian Science Fund (FWF) under grant W800-N05. The third author (PG) acknowledges a grant of the TU graduate school *Partial Differential Equations in Technical Systems — Modeling, Simulation, and Control* funded by Vienna University of Technology. The

research of the other authors is supported through the FWF project *Adaptive Boundary Element Method*, funded by the Austrian Science Fund (FWF) under grant P21732.

References

[1] M. Ainsworth, J.T. Oden, A posteriori error estimation in finite element analysis, Wiley-Interscience [John Wiley & Sons], New-York, 2000.

[2] M. Aurada, M. Ebner, S. Ferraz-Leite, M. Mayr, P. Goldenits, M. Karkulik, D. Praetorius, `HILBERT` — A Matlab implementation of adaptive BEM, ASC Report 44/2009, Institute for Analysis and Scientific Computing, Vienna University of Technology, Wien, 2009, software download at `http://www.asc.tuwien.ac.at/abem/hilbert/`

[3] M. Aurada, S. Ferraz-Leite, D. Praetorius, Estimator reduction and convergence of adaptive FEM and BEM, ASC Report 27/2009, Institute for Analysis and Scientific Computing, Vienna University of Technology, Wien 2009.

[4] M. Aurada, P. Goldenits, D. Praetorius, Convergence of data perturbed adaptive boundary element methods, ASC Report 40/2009, Institute for Analysis and Scientific Computing, Vienna University of Technology, Wien 2009.

[5] R. Bank, Hierarchical bases and the finite element method, Acta Numerica 5 (1996) 1–45.

[6] P. Binev, W. Dahmen, R. DeVore, Adaptive finite element methods with convergence rates, Numer. Math. 97 (2004) 219–268.

[7] C. Carstensen, An a posteriori error estimate for a first-kind integral equation, Math. Comp. 66 (1997) 69–84.

[8] C. Carstensen, D. Praetorius, Averaging techniques for the effective numerical solution of Symm's integral equation of the first kind, SIAM J. Sci. Comp. 27 (2006) 1226–1260.

[9] C. Carstensen, D. Praetorius, Averaging techniques for the a posteriori BEM error control for a hypersingular integral equation in two dimensions, SIAM J. Sci. Comput. 29 (2007) 782–810.

[10] C. Carstensen, D. Praetorius, Averaging techniques for a posteriori error control in finite element and boundary element analysis, in: Boundary Element Analysis: Mathematical Aspects and Applications (M. Schanz, O. Steinbach eds.), Springer Lect. Notes Appl. Comput. Mech. 29 (2007) 29–59.

[11] C. Carstensen, D. Praetorius, Convergence of adaptive boundary element methods, ASC Report 15/2009, Institute for Analysis and Scientific Computing, Vienna University of Technology, 2009.

[12] J. Cascon, C. Kreuzer, R. Nochetto, K. Siebert, Quasi-optimal convergence rate for an adaptive finite element method, SIAM J. Numer. Anal. 46 (2008) 2524–2550.

[13] P. Deuflhard, P. Leinen, H. Yserentant, Concepts of an adaptive hierarchical finite element code, IMPACT Comput. in. Sci. and Eng. 1 (1989) 3–35.

[14] W. Dörfler, A convergent adaptive algorithm for Poisson's equation, SIAM J. Numer. Anal. 33 (1996) 1106–1124.

[15] C. Erath, S. Ferraz-Leite, S. Funken, D. Praetorius, Energy norm based a posteriori error estimation for boundary element methods in two dimensions, Appl. Numer. Math. 59 (2009) 2713–2734.

[16] C. Erath, S. Funken, P. Goldenits, D. Praetorius, Simple error estimators for the Galerkin BEM for some hypersingular integral equation in 2D, ASC Report 20/2009, Institute for Analysis and Scientific Computing, Vienna University of Technology, Wien 2009.

[17] S. Ferraz-Leite, C. Ortner, D. Praetorius, Convergence of simple adaptive Galerkin schemes based on $h - h/2$ error estimators, Numer. Math., published online first (2010).

[18] S. Ferraz-Leite, D. Praetorius, Simple a posteriori error estimators for the h-version of the boundary element method, Computing 83 (2008) 135–162.

[19] I. Graham, W. Hackbusch, S. Sauter, Finite elements on degenerate meshes: Inverse-type inequalities and applications, IMA J. Numer. Anal. 25 (2005) 379–407.

[20] W. Hackbusch, Hierarchische Matrizen (in German), Springer, Berlin 2009.

[21] E. Hairer, S. Nørsett, G. Wanner: Solving ordinary differential equations I. Nonstiff problems, Springer, New York, 1987.

[22] N. Heuer, M. Mellado, E. Stephan, hp-adaptive two-level methods for boundary integral equations on curves, Computing 67 (2001) 305–334.

[23] M. Maischak, The analytical computation of the Galerkin elements for the Laplace, Lamé and Helmholtz equation in 2D BEM, Technical Report, Institute for Applied Mathematics, University of Hannover (1999).

[24] M. Maischak, P. Mund, E. Stephan: Adaptive multilevel BEM for acoustic scattering, Comput. Methods Appl. Mech. Eng. 150 (2001) 351–367.
[25] W. McLean, Strongly elliptic systems and boundary integral equations, Cambridge University Press, Cambridge, 2000.
[26] P. Morin, K. Siebert, A. Veeser, A basic convergence result for conforming adaptive finite elements, Math. Models Methods Appl. Sci. 18 (2008) 707–737.
[27] P. Mund, E. Stephan, J. Weiße: Two-level methods for the single layer potential in $\mathbb{R}^3$, Computing 60 (1998) 243–266.
[28] G. Of, O. Steinbach, P. Urthaler, Fast evaluation of Newton potentials in the boundary element method, Preprint 2008/3, Institute for Numerical Mathematics, Graz University of Technology, 2008.
[29] S. Sauter, C. Schwab, Randelementmethoden: Analyse, Numerik und Implementierung schneller Algorithmen (in German), Teubner Verlag, Wiesbaden, 2004.
[30] O. Steinbach, Numerical approximation methods for elliptic boundary value problems: Finite and boundary elements, Springer, New York 2008.
[31] R. Stevenson, Optimality of a standard adaptive finite element method, Found. Comput. Math. 7 (2007) 245–269.
[32] R. Stevenson, The completion of locally refined simplicial partitions created by bisection, Math. Comp. 77 (2008) 227–241.
[33] R. Verfürth, A review of a posteriori error estimation and adaptive mesh-refinement techniques, Wiley-Teubner, 1996.

Institute for Analysis and Scientific Computing, Vienna University of Technology, Wiedner Hauptstrasse 8-10, A-1040 Wien, Austria